This is an Accepted Manuscript of an article published by Taylor & Francis in **CRITICAL REVIEWS IN ENVIRONMENTAL SCIENCE AND TECHNOLOGY** on 04.02.2021, available online: https://www.tandfonline.com/doi/full/10.1080/10643389.2021.1877032

Postprint of: Gontarek-Castro E., Castro-Muñoz R., Lieder M., New insights of nanomaterials usage toward superhydrophobic membranes for water desalination via membrane distillation: A review, CRITICAL REVIEWS IN ENVIRONMENTAL SCIENCE AND TECHNOLOGY (2021), DOI: 10.1080/10643389.2021.1877032

New insights of nanomaterials usage toward superhydrophobic membranes for water desalination via membrane distillation: A review

AQ0

AQ20 Emilia Gontarek[a] Roberto Castro-Muñoz[b] Marek Lieder[a]

[a]Faculty of Chemistry, Department of Process Engineering and Chemical Technology, Gdansk University of Technology, Gdansk, Poland; AQ1

[b]Tecnologico de Monterrey, Campus Toluca, Avenida Eduardo Monroy Cárdenas 2000 San Antonio Buenavista, Toluca de Lerdo, Mexico

CONTACT Emilia Gontarek emilia.gontarek@pg.edu.pl; Roberto Castro-Muñoz food.biotechnology88@gmail.com; castromr@tec.mx AQ2

Abstract

Membrane distillation (MD) is a promising technology for seawater desalination due to the ability to process high-salinity waters and the ability to be driven by low-grade or waste heat. However, practical applications of MD membranes are limited by the low vapor flux and fouling problem. Recently, there is a growing interest in developing novel MD membrane materials with enhanced hydrophobicity to improve the efficiency of desalination performance. Interestingly, the incorporation of nanomaterials for tailoring superhydrophobic properties of MD membranes has attracted enormous attention in MD. Herein, according to the new insights of the available literature data, the current trend for achieving superhydrophobic MD membranes by embedding inorganic nanomaterials is provided. The influence of the inorganic additives on membrane fouling, stability, separation performance, is also discussed. Finally, theoretical principles of MD, the milestones of the evolution of developing superhydrophobic membrane surfaces, and future trends are also given for the new readers in the field.

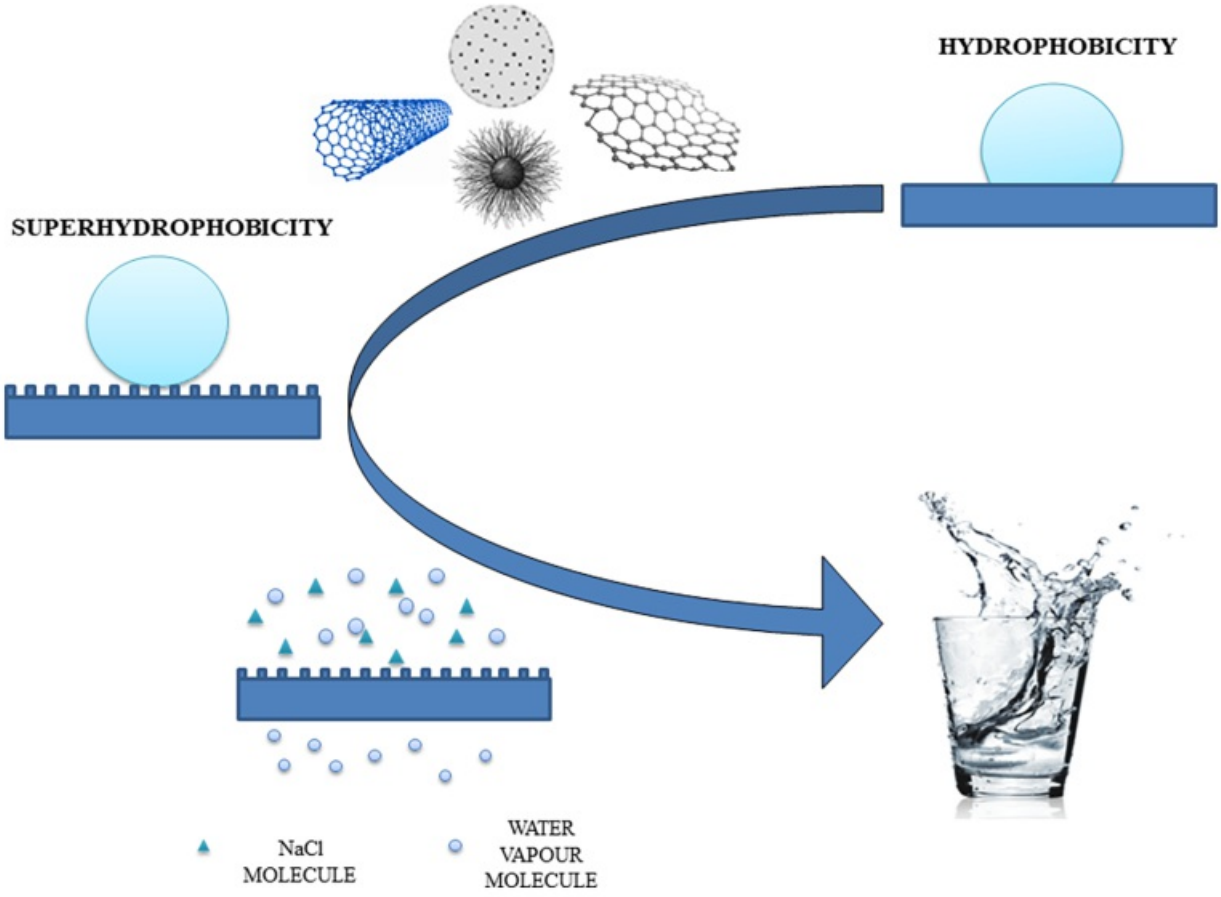

Keywords: Desalination; membrane distillation; nanomaterials; superhydrophobic membranes; vapor transport; water treatment

1. Introduction

Membrane distillation is a thermally-driven process, which is known for its high potential for water treatment. Briefly, the real possibility of application, especially in seawater desalination processes, regards to its high water recovery and ability to treat high-salinity waters. Although, reverse osmosis is the most energy efficient desalination technology, membrane distillation has the potential to become less energy intensive by incorporating low grade energy or waste heat (Deshmukh et al., 2018). In particular, MD process requires the use of hydrophobic micro-porous membrane, which separates two different aqueous solutions but allows only vapor permeation. The driving force of the process is the vapor pressure difference across the membrane, which is induced by the temperature difference between feed and permeate. In principle, due to membrane hydrophobicity, vapor is the only one able to pass through the membrane pores, making MD a good candidate for the separation of nonvolatile compounds from water solution. When dealing with seawater desalination, the most typical configuration is direct contact membrane distillation (DCMD), in which hydrophobic micro-porous membrane is directly exposed to both streams (i.e. heated feed and cold permeate), as illustrated in Figure 1. Typically, both streams are operated in a counterflow configuration. It is worth to mention that DCMD configuration owes its popularity to the easy construction, while in fact its performance is less efficient than other configurations e.g. air gap membrane distillation (AGMD) and vacuum membrane distillation (VMD). For instance, Eykens et al. (2017) stated that AGMD configuration modules showed a higher flux and lower energy consumption compared to direct contact membrane distillation (DCMD) in a pilot scale experiments, while Cerneaux et al. (2009) observed much higher fluxes of VMD than DCMD during desalination using ceramic membranes.

Figure 1. The scheme of direct contact membrane distillation (DCMD).

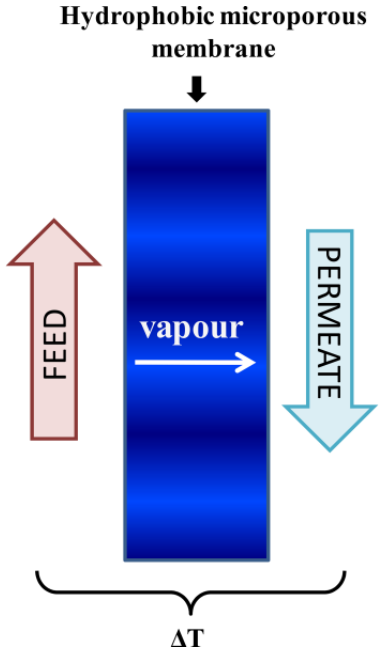

For an efficient operation of a MD process, the perm-selective barrier should present a highly hydrophobic surface, which is preferred since it may concurrently repel the water molecules in liquid state and favor the vapor transport. For this reason, superhydrophobic membranes gained special attention in MD process. Such a term implies to those membranes that may display a high water contact angle (over 150°). However, most of the membrane materials do not display such a high contact angle, as shown in Table 1.

Table 1. Some examples of hydrophobic membrane materials and their water contact angles.

Membrane	Chemical structure	Water contact angle	References
PVDF (GE Osmonics)	$(CH_2CF_2)_n$	113o	Zhang et al. (2010)
Nanofibrous PVDF	$(CH_2CF_2)_n$	>135o	Liao, Wang et al. (2013a)
PTFE (Membrane Solutions)	$(CF_2CF_2)_n$	126o	Zhang et al. (2010)
PP (Membrana GmbH)	$[CH_2CH(CH_3)]_n$	98o	Gryta (2008)
Matrimid 5218	3,3′-4, 4′-benzophenone tetracarboxylic-dianhydride diaminophenylindane	85o	Francis et al. (2013)
Nanofibrous Matrimid	3,3′-4, 4′-benzophenone tetracarboxylic-dianhydride diaminophenylindane	130o	Francis et al. (2013)
Nanofibrous polystyrene	$[CH_2CH(C_6H_5)]_n$	114o	Ke et al. (2016)
Polysulfone	$[C_6H_4\text{-}4\text{-}C(CH_3)_2C_6H_4\text{-}4\text{-}OC_6H_4\text{-}4\text{-}SO_2C_6H_4\text{-}4\text{-}O]_n$	106o	Peng et al. (2013)
Hyflon AD	$(C_4F_6O_3)n(C_2F_4)_m$	130–150o	Gugliuzza et al. (2006)

For this reason, there is a growing trend in developing new strategies for improving the existing materials, as well as

tailoring new materials, to obtain superhydrophobic membranes. For instance, Figure 2 depicts the growing interest of researchers in exploring superhydrophobic membranes over the last 10 years.

Figure 2. Publication trend on developing superhydrophobic membranes over the last 10 years (source Web of Science, Keywords: superhydrophobic membrane).

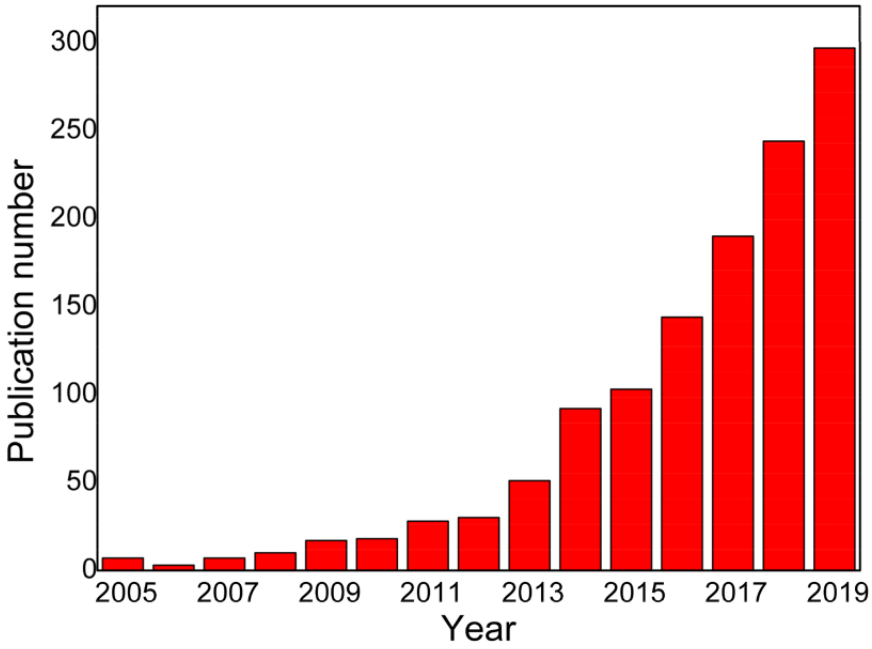

Furthermore, few review papers dedicated to membranes for MD application have been published within the last years. Eykens et al. (2017) provided a literature review on the different methods for MD membranes synthesis including basic process principle, parameters evaluation and module types used for MD. Himma et al. (2019) focused on the preparation methods of only superhydrophobic membrane, including direct processing method and surface modification. Nthunya, Gutierrez, Derese et al. (2019a) provided a comprehensive review regarding MD process, additionally, some examples of membrane modification by incorporation of nanoparticles were discussed. Pan et al. (2019) reviewed electrospun nanofibrous membranes for MD applications, emphasized on the research developments in recent 3 □ 4 years. An analysis on the relationship between the membrane structures and the MD performance has been provided. Yao et al. (2020) focused on various types of surface special wettability, and their fabrication methods for MD. Nevertheless, most of the above mentioned works were mainly devoted to methods of membrane preparation and synthesis. Considering the recent updates in MD regarding the role of nanomaterials in tailoring membrane morphology and water vapor transport during desalination, we believe that it is necessary to organize a new review paper that will emphasize the effect of these materials on membrane performance through the state-of-the-art research development discussion. Therefore, this paper brings and elucidates the recent literature review on strategies adopted by the research community in fabricating superhydrophobic MD membranes for desalination, giving special attention to polymeric membranes containing different nanomaterials. An overview of the typical and emerging nanomaterials used for MD membranes modification as well as the underlying mechanism leading to improvement of MD performance has been introduced. In addition to this, we provide the theoretical principles and requirements for MD membranes.

2. Theoretical principles of MD process

2.1. Mass transfer

Within membrane distillation process, the mass transfer takes place due to the vapor pressure gradient between feed and permeate. First, volatile species are transported from the bulk feed to the membrane surface, subsequently such compounds diffuse through the membrane pores in gaseous phase; finally, the gaseous volatiles are transported from the permeate membrane surface to the bulk permeate. To date, the mass transfer during MD has been described by four possible mechanisms: Knudsen diffusion, viscous flow, surface diffusion and molecular diffusion (Orfi et al., 2016). In general, for DCMD process, viscous flow and surface diffusion can be omitted (Lawson & Lloyd,1997), while for some specific cases the models can be further simplified depending on the pore size, as described below (Khayet et al., 2004).

1. Knudsen diffusion model: systems where collisions between molecule and pore wall are dominant, as denoted by Eq. (1):

$$N' = \frac{1}{RT}\frac{2\,\epsilon r}{3\tau}\left(\frac{8RT}{\pi M_i}\right)^{1/2}\frac{(p_1 - p_2)}{\delta} \quad (1)$$

where ε, r, τ, M_i and δ are porosity, pore radius, tortuosity, molecular weight of water vapor and membrane thickness, respectively.

2. Molecular diffusion model: systems, where the membrane pore size is relatively large, the mass transfer is mainly determined by the collisions between the molecules:

$$N' = \frac{\epsilon}{\tau\delta}\frac{PD_{ij}}{RT}\frac{(p_1 - p_2)}{|p_a|_{ln}} \quad (2)$$

where D, P and p_a are the Fick's diffusion coefficient, total pressure in the pore and air pressure in the pore, respectively.

During MD operation the concentration of solutes in feed solution becomes higher at the liquid/gas interface than in the bulk feed. This phenomenon is called concentration polarization. Concentration polarization coefficient (CPC) is given by Eq. (3):

$$CPC = \frac{c_{f,m}}{c_f} \quad (3)$$

where $c_{f,m}$ is a concentration of the solute at the membrane surface and c_f is a concentration of the solute in the bulk feed.

2.2. Heat transfer

Along with the mass, the heat transfer also occurs. Heat transfer represents an important aspect in all MD configurations. For instance, the heat transfer in DCMD is usually considered in two important mechanisms (Alkhudhiri et al., 2012). The conductive heat transfer along the membrane pores that occurs together with the vapor diffusion causes temperature change at the both membrane boundary layers. This leads to a temperature gradient in the feed and permeate (between the bulk and boundary layer) and results in the convective heat transfer (Srisurichan et al., 2006).

Convective heat transfer at the feed boundary layer can be given by Eq. (4):

$$Q_f = h_f(T_f - T_{f,s}) \quad (4)$$

while for permeate at the boundary layer:

$$Q_p = h_p(T_{p,s} - T_p) \quad (5)$$

In the case of the heat transfer across the membrane, it can be denoted by Eq. (6):

$$Q_m = h_m(T_{f,s} - T_{p,s}) + J\Delta H_v \quad (6)$$

where h_f, h_p and h_m represent the heat transfer coefficients of the feed, permeate and membrane, respectively, T_f and T_p are the temperature of the feed and permeate, respectively. $T_{f,s}$ and $T_{p,s}$ are the surface temperatures on the feed and permeate side, respectively.

With the increasing difference between the bulk feed and permeate temperatures, as well as the surface temperature at the corresponding side of the membrane, the effect of temperature polarization also raises (Termpiyakul et al., 2005). Temperature polarization (ψ) is defined as follows:

$$\psi = \frac{T_{f,s} - T_{p,s}}{T_f - T_p} \quad (7)$$

Such equation relates to the effect of heat transfer at the boundary layer and the total heat transfer resistance for a given system. When the ψ value reaches 1, the resistances of thermal boundary layer are reduced, while when the value is equal to 0, the system is controlled by large thermal boundary layer resistance. Typically, for DCMD temperature polarization value lies between 0.4 and 0.7 (Curcio & Drioli, 2005).

2.3. Fouling phenomena

The fouling is defined as the deposition of any material on the membrane surface or in the membrane pores, that leads to a meaningful change in the membrane separation performance (Smolders & Franken, 1989). The fouling in MD can occur in various forms depending on the chemical composition of the feed bulk solution including organic, inorganic, and biological fouling. In MD processes, mineral scaling is usually referred to inorganic fouling. For example, during desalination of concentrated salt solutions, it is common to observe scale formation at the membrane surface (Kullab & Martin, 2011). There are different ions in hypersaline wastewaters that may form sparingly soluble minerals, such as sulfates, carbonates, and silicates. During MD process, the feed solution get concentrated as water evaporates, leading in some cases to the growth of a layer of mineral crystals on the membrane surface (He et al., 2008). Organic fouling rises from treatment of solutions containing protein-type macromolecules, humic acids, or emulsified oil droplets, that leads to their adsorption at the membrane surface (Hausmann et al., 2013). Biological fouling (biofouling) is caused by the growth of bacteria, fungi, and algae, also called as a biofilm formation on the membrane surface. In general, fouling increases the resistance to heat and mass transfer, and leads to the rapid flux decline and membrane wetting (Goh et al., 2013). To improve the MD stability against different fouling types, membranes with special surface wettability, such as Janus, ~~O~~omniphobic and ~~S~~superhydrophobic have been developed (Yao et al., 2020).

3. Membrane requirements for MD process

It has been documented that MD process operates with lower temperatures and pressures compared to other membrane processes for water desalination (e.g. reverse osmosis). In addition to this, MD is characterized by a high salt rejection rates, and lower tendency to concentration polarization phenomena (Macedonio & Drioli, 2008). The limiting factor for the development of a more efficient MD process is the lack of suitable membrane materials. This efficiency will be ensured when the membrane will be free from pore blocking and wetting. However, the feed solution during MD sea water desalination may contain substances, such as organic matter and oil particles, that promote fouling and wetting of conventional hydrophobic membranes. Moreover, the treatment of hypersaline brine results in mineral scaling on the membrane surface that leads to significant flux reduction, while the presence of low surface tension liquids in the feed reduces the overall surface tension of the feed and results in pore wetting. For this reason, the technology of MD membrane preparation faces few challenges including pore wetting, mineral scaling, and membrane fouling (Horseman et al., 2021). Several studies have been devoted to~~in~~ the preparation of synthetic membranes that would meet all of the requirements of MD process. So far, the most popular membrane materials for MD process are stretched or phase inverted polymers, such as polypropylene (PP) (Tang et al., 2010), polytetrafluoroethylene (PTFE) (Zhu et al., 2013) and poly (vinylidene fluoride) (PVDF) (Devi et al., 2014). Ceramic materials are less used since they display high thermal conductivity, leading to heat loss through the membrane (Wang et al., 2016). Furthermore, ceramic-based materials are usually more expensive than polymeric ones. According to these disadvantages, few development works using ceramic membranes have been reported (Cerneaux et al., 2009; Fang et al., 2012; Larbot et al., 2004). Therefore, special emphasis has been paid over the last years at improving polymeric membranes. Nevertheless, several works have addressed unreliability of the polymeric membranes in long-term operations (Jeong et al., 2016; Khayet et al., 2005). For this reason, there is a need to improve some physical and chemical properties, including pore size, contact angle, porosity, and thermal conductivity. These properties directly affect membrane separation performance in terms of energy efficiency (heat loss through the membrane), stability, retention and flux (Eykens et al., 2017). Therefore, to fill this gap on the membrane market, there is a need to develop MD membranes with high mass transfer, excellent anti-wetting and anti-fouling properties, chemical inertness, and low cost.

As the MD membranes are contactors between two phases, they must possess a hydrophobic layer, which prevents the wetting provoked by the feed solution and concurrently provide retention of nonvolatile solutes. The use of a superhydrophobic membrane can significantly improve MD efficiency, this phenomenon is described in detail in next sections. To evaluate the membrane susceptibility to wetting, the liquid entry pressure (LEP) parameter must be determined. LEP is defined as the pressure value that is required for the liquid to pass through the membrane. According to the literature, for a proper operation of MD plant, LEP of the feed solution should be above 2.5bar (Schneider et al., 1988). LEP is described based on Laplace equation:

$$LEP_w = \frac{B\gamma_L \cos\theta}{r_{max}} \quad (8)$$

where B is a geometric factor of pore structure (equal to 1 for cylindrical pores), γ_L is the surface tension of the liquid, θ is the liquid/membrane contact angle and r_{max} is the maximum pore size (Franken et al., 1987). As a result, to achieve high LEP, membrane material should have small pore size, high surface tension and low interface energy between membrane and liquid.

Another important parameter for the optimal membrane performance is its thickness. Membrane thickness significantly affects the vapor flux through the membrane. Thicker membrane increases the mass transfer resistance, and thus reduces the vapor flux. On the other hand, thicker membrane reduces the heat loss. To date, several studies indicate that the optimal membrane thickness for a MD membrane should be in the range of 30–60 µm (Laganà et al.,

2000). However, it is important to point out that this value may vary depending on the feed concentration, process conditions and membrane properties. In addition to this, the membrane porosity determines the process efficiency. Porosity is defined as the relationship of the volume of the pores and the total volume of the membrane. Membrane porosity is proportional to the evaporation surface area, and consequently, higher porosity membranes have higher vapor flux. According to the literature, the suggested membrane porosity value for an efficient MD should range from 30 to 85% (El-Bourawi et al., 2006). Knowing the densities of membrane and membrane material, the porosity can be calculated with the method proposed by Smolders and Franken (Smolders & Franken, 1989):

$$\epsilon = 1 - \frac{\rho_m}{\rho_{mat}} \tag{9}$$

Furthermore, it has been also reported that higher porosity reduces conductive heat loss, this is due to the fact that the gases filling the pores of the membrane are less heat conductive than polymeric membrane materials (El-Bourawi et al., 2006). The pore features also influence the MD process, e.g. one of these parameters concerns the deviation of the pore shape from the cylindrical structure, which is called membrane tortuosity (τ). In theory, for a higher vapor flux, lower tortuosity is desired (Srisurichan et al., 2006). There is a direct correlation between porosity and tortuosity value, that can be calculated with the following equation proposed by Mackie and Meares (Mackie & Meares, 1955):

$$\tau = \frac{(2-\epsilon)^2}{\epsilon} \tag{10}$$

As mentioned previously, microporous membranes are usually needed for MD application. However, a slight variance regarding an optimal pore size can be found in the literature. For instance, Schneider et al. (1988) have reported that for pore flooding prevention, a maximum pore diameter should be in the range 0.5–0.6 μm, while El-Bourawi et al. (2006) noted that this range can be extended to 0.1–1 μm. Although for bigger pores higher fluxes are expected, it has been also reported that too large pore dimensions cause membrane wettability. Nevertheless, to estimate the optimal pore size, the surface tension of the feed solution must be taken into account.

As the driving force of the process is temperature difference, an important aspect during membrane designing is the conductivity of the membrane material. Less heat loss during the process leads to higher energy efficiency and less susceptibility to temperature polarization phenomena, thus improved flux through the membrane can be obtained. Thermal conductivities of most often used polymers for MD membranes, such as PP, PTFE, PVDF, are similar to each other, ranging from 0.11 for PP up to 0.27 $Wm^{-1}K^{-1}$ for PTFE at 23 °C (Alkhudhiri et al., 2012).

4. Toward the enhancement of hydrophobicity

The history of superhydrophobic surfaces studies dates back to the early 20th century when Ollivier (1907) observed the contact angles of nearly 180°, long before membrane distillation has been patented (Bodell, 1963) (see Figure 3). Nevertheless, first artificial superhydrophobic surfaces have been reported and demonstrated by Onda et al. (1996) and it was the beginning of the development of various methods for superhydrophobic surfaces preparation. In 2009, materials with a contact angle above 150° started to be implemented for MD membranes (Zeyu et al., 2009).

Figure 3. Timeline of MD and superhydrophobic surface developments (Findley, 1967; Ma et al., 2005).

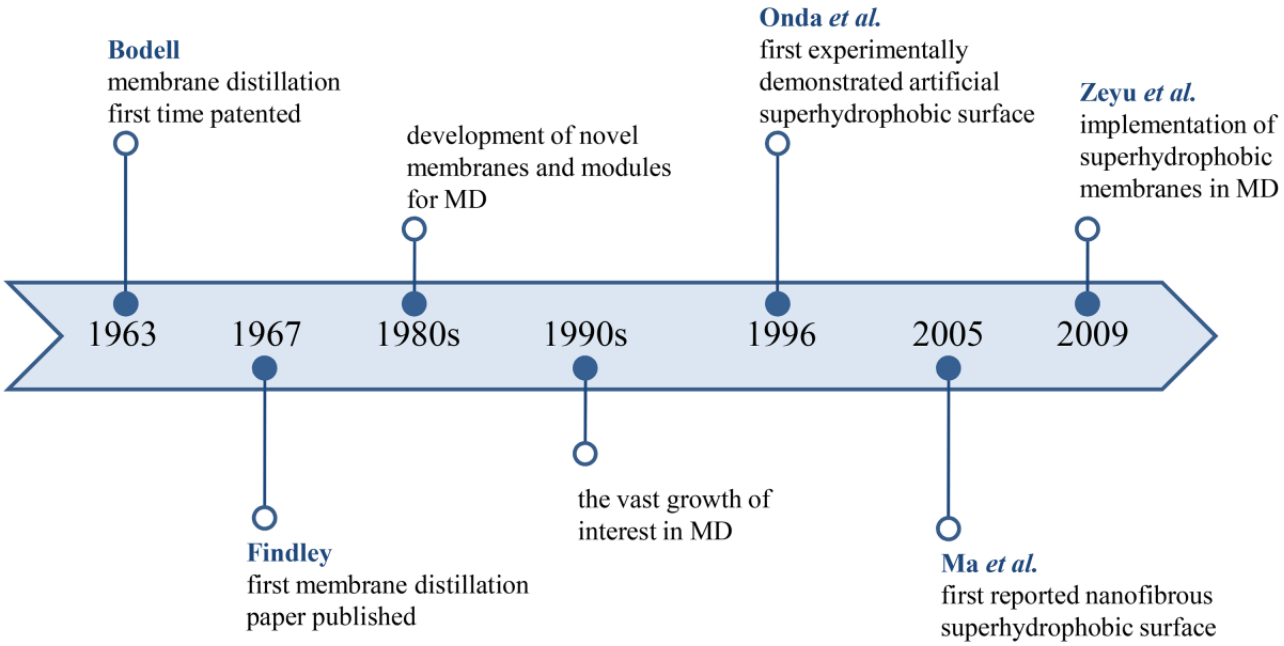

The phenomena of surface wetting by a liquid and its physicochemical~~physiochemical~~ principle have been already well studied. A droplet resting on a solid surface can take a form of equilibrated shape and remain on the surface as a droplet or spread into a thin layer on the material surface. The behavior of the droplet depends on three thermodynamically balanced interfacial tensions that relate to the existence of an interface between liquid and vapor, solid and liquid and solid and vapor (Shirtcliffe et al., 2010). The wettability of the solid surface is ~~dominated~~ mainly dominated by its chemical composition and structure.

The design of superhydrophobic surface ha~~ve~~s been inspired by the structure of lotus leaves with a contact angle in excess of 150° and self-cleaning properties. This effect can be achieved by creating a rough and hydrophobic surface. The roughness enhances the contact angle of hydrophobic surfaces well beyond that possible to achieve by chemistry itself (McHale et al., 2004). This was well described by Wenzel equation (11) (Wenzel, 1936):

$$\cos\theta_r = r\cos\theta_e \quad (11)$$

where r is a roughness factor, θ_r is a contact angle on a rough surface, and θ_e is Young's equilibrium contact angle. According to the Wenzel's equation, the surface roughness amplifies the effect of the surface chemistry which in this equation is determined as $\cos\theta_e$. The equation shows that for hydrophilic surfaces with $\theta < 90°$, the roughness factor enhancement will cause further reduction of the Wenzel contact angle toward 0°, whereas for hydrophobic surfaces with $\theta > 90°$, it will lead to further increase of the Wenzel contact angle toward 180°. Nevertheless, the Wenzel equation is limited to the homogeneous rough surface, and it was extended by Cassie and Baxter in 1944 (Cassie & Baxter, 1944). Cassie-Baxter equation applies for the porous membrane with a heterogeneous surface. In this case, the presence of the air in the pores of the material prevents the pores from being filled with liquid and liquid only bridges between the solid surface. Although the surface is topographically structured, the roughness factor does not directly enter into the Cassie–Baxter equation (12):

$$\cos\theta_{CB} = f_1\cos\theta_e - (1 - f_1) \quad (12)$$

where θ_{CB} is heterogeneous contact angle, f_1 is a fraction of the contact line of liquid with the solid, thus $(1-f_1)$ is the area bridged between solid surface features. According to Cassie-Baxter equation, θ_{CB} will increase with the decrease of f_1. It means that to enhance the hydrophobicity of the surface the contact line of liquid with the solid has to be minimized. Thus, the roughness indirectly matters because it determines the solid surface fraction. Thus, a Cassie − Baxter state is one in which the liquid does not penetrate into the hollows of the rough surface but remains suspended on top of the surface protrusions (see Figure 4B), while in Wenzel state the liquid is in contact with the entire exposed surface of the solid (Figure 4A) (Giacomello et al., 2012).

Figure 4. Scheme of the A) Wenzel and B) Cassie − Baxter state for a droplet.

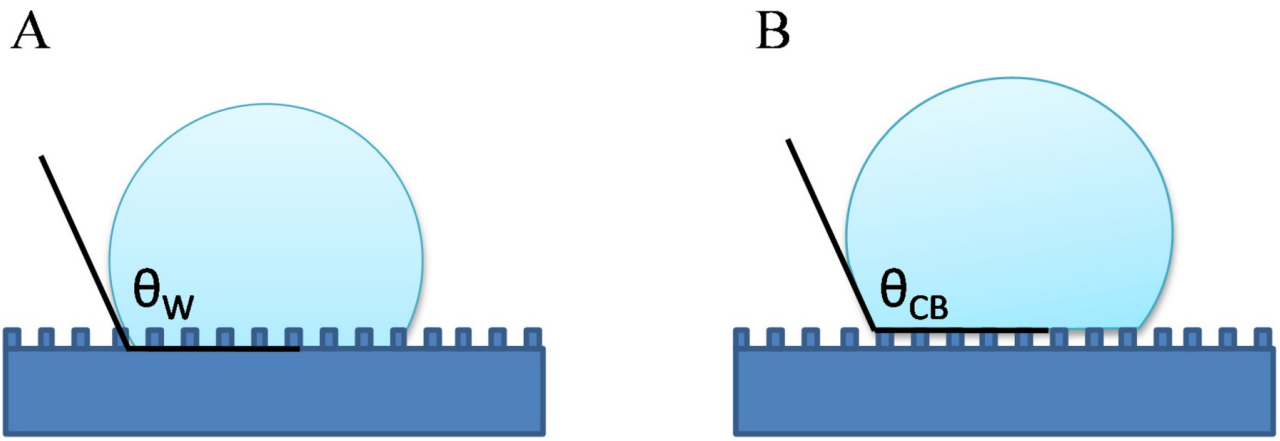

4.1. Different approaches for hydrophobicity enhancement

There are different ways for wettability diminishment that are usually based on the combination of surface patterning and surface modification technologies starting from the chemical modification (Ogawa et al., 2007), electrospinning (Liao, Wang et al., 2013a), nanocomposite preparation (Tijing et al., 2016), sol-gel approach (Zhang & Wang, 2013) through nanoparticles coating (Chen et al., 2018; Razmjou et al., 2012; Shao et al., 2019), surface silanization (Boo et al., 2016) and plasma fluorination (Yang et al., 2014, 2015). A summary of various approaches used for hydrophobicity enhancement is given in Table 2.

Table 2. Different approaches for hydrophobicity enhancement.

Strategy used	Polymer type	Initial contact angle (°)	Final contact angle (°)	LEP	References
CF_4 plasma treatment	PVDF	137	162.5	–	Yang et al. (2015)
Spray deposition of PDMS/SiO_2 nanoparticles mixture	PVDF	107	156	275 kPa	Zhang et al. (2013)
Modification with fluorinated silica layer	PEI	66.7	124.8	–	Zhang and Wang (2013)
Dispersion of detonation nanodiamonds	PVDF	110	119	–	Bhadra et al. (2014)

Strategy used	Polymer type	Initial contact angle (°)	Final contact angle (°)	LEP	References
Clay nanocomposite formation	PVDF	128	154.2	200 kPa	Prince et al. (2012)
SiO_2 coating and fluorination	PP	120	150	–	Shao et al. (2019)
Electrospinning of PVDF-silica layer	PVDF	135	>150	150 kPa	Liao, Wang et al. ~~et al.~~ (2014~~a~~)
Chemical modification with perfluoropolyether	PVDF	88	115	390 kPa	Yang et al. (2011)
Coagulation bath with N-methylpyrrolidone	PSf	105	144	260 kPa	Tian et al. (2015)

The hydrophobicity of the uniform polymeric structures is usually not sufficient for MD process. In practice, the enhancement of the observed surface hydrophobicity is based on increasing the surface roughness and lowering solid/liquid interface energy. According to the literature (Takashi et al., 1999), an effective way for lowering solid/liquid interface energy is its functionalization by fluorinated alkyl units, however, there is a certain limitation in hydrophobicity improvement of smooth surfaces. For example, in the case of smooth PVDF, a surface that is saturated by fluorinated methyl groups, it is possible to reach a maximum 120° contact angle (Yue et al., 2013). Therefore, the enhancement of the surface hydrophobicity is based on increasing the surface roughness (Li et al., 2007). Thus, to achieve a strong water repellent rough membrane, a proper modification has to be adopted focusing on the creation of micro- and nanostructured surface, as shown in the Figure ~~4~~5. In such approach, the authors obtained complex topography via depositing TiO_2 nanoparticles on microporous PVDF membranes (Razmjou et al., 2012). Due to the Cassie-Baxter model (Cassie & Baxter, 1944), capillary forces may inhibit or reduce the penetration of the liquid into the rough and complex surface. As a result, water droplets sit upon the top of surface protrusions and air gaps rather than follow the surface contours. In the case of multilevel roughness, there is an unusually strong water-repellency on the surfaces due to the increase in the number of sharp and narrow protrusion that are in contact with water droplet. In other words, the increase of surface roughness reduces the contact area between liquid and solid and as a consequence reduces the adhesion of a droplet to the solid surface.

A facile way to fabricate membranes with rough surfaces is electrospinning technique. Electrospinning of polymers allows fabricating nanofiber membranes. During electrospinning process, polymeric solution is exposed to the electric field. When the applied electrostatic force overcome the surface tension, a so called fiber jet is ejected, followed by the rapid evaporation of the solvents and the fiber deposition on the collector (Reneker & Yarin, 2008). Thanks to the presence of microscale and nanoscale fibers in the structure, the electrospun membranes are highly porous and have high surface-to-volume ratio and three-dimensional interconnected structure. Such particular structure and ease of preparation made electrospun membranes to promote their applications in various fields, such as filtration (Wang et al., 2012), fuel cell technology (Tamura & Kawakami, 2010) and tissue engineering (Bhattarai et al., 2004). One of the advantages of electrospinning is the diversity of the polymers that can be used for fabrication MD membranes in contrary to commercial MD membrane synthesis that is limited to the polymers such as PVDF, PP, PTFE (as mentioned in previous section). As an example, styrene–butadienestyrene (SBS) has been recently electrospun into nanofibrous MD membrane (Duong et al., 2018). Results showed that SBS electrospun membrane exhibited higher hydrophobicity compared to the commercial PTFE membrane. A common method for further roughness enhancement and hierarchical structure creation is an addition of hydrophobic nanomaterials, such as graphene, CNTs or silica nanoparticles into electrospinning dope solutions (Liao, Wang et al., 2014~~a~~; Tijing et al., 2016; Woo, Tijing et al., 2016). For instance, Tijing et al. (2016) added different concentrations (1–5 wt%) of carbon nanotubes (CNTs)

into the PcH dope solution for electrospinning. With CNTs concentration of 5wt%, the nanofiber membranes obtained a very high contact angle of 158.5° and high LEP of 99kPa due to presence of CNTs in/on the nanofibers which produced beads on the surface of the membrane leading to increased roughness. An effective method to functionalize electrospun membranes is electrospraying in order to cover the nanofibrous membrane with inorganic/organic micro/nano particles. The combination of electrospinning and electrospraying was used to fabricate PcH nanofibrous membrane functionalized with TiO_2 nanoparticles (Seyed Shahabadi et al., 2017). The contact angle increased from 142° up to 162° after electrospraying.

4.2. Incorporation of inorganic nanomaterials

Different studies have shown that the incorporation of nanofillers into polymers could tune the structure and physicochemical properties of membranes, such as hydrophobicity but also porosity, surface charge density, chemical, thermal and mechanical stability (Castro-Muñoz, Ahmad & Fila ~~et al.~~, 2019; Yin & Deng, 2015). Recently, the use of several inorganic materials, such as carbon nanotubes, graphene, clay, silica and titanium dioxide, has become a new trend for superhydrophobic MD membranes preparation.

4.2.1. Graphene-based materials

It is likely that graphene-based materials are currently among the most deeply explored additives. Graphene has attracted considerable attention for water treatment and purification processes, especially for pressure-driven membrane processes, and the advantages of its use have been proven both by molecular simulations (Cohen-Tanugi & Grossman, 2012) and experimental studies (Han et al., 2013). To the date, different mechanisms of selective permeation of graphene and graphene oxide have been proposed, e.g. Nair et al. (2012) suggested a network of parallel channels between stacked graphene oxide layers (see Figure ~~5~~6). Such channels are arranged perpendicularly to a mass transport vector. The bottom and ceiling of these channels are usually permeable to water or ions due to presence of holes in them. It has been documented that, even when the mixture of water and other compounds (e.g. gases and liquids) was fed, the water permeation rate could be at least five orders of magnitude higher than that of the other component (Castro-Muñoz, Buera-González et al., 2019). The presence of nanochannels in membrane structure together with different chemical interactions, that occurs between the transported ions and oxygen functional groups, are responsible for the selective permeation of GO membranes (Sun et al., 2013). According to Joshi et al. (2014), nanochannels in graphene oxide structure can open up only in the hydrated state, and the sieving properties of GO may depend on the humidity of the surroundings as this parameter defines the interlayer spacing. The water molecules intercalation between single GO sheets causes the swelling of the layer. It is mentioned that the interlayer spacing can reach the value of 13.5 Å, and concurrently makes the membrane permeable to most of the hydrated ions (as the diameter of most of the hydrated ions is smaller than 13.5 Å) (Abraham et al., 2017). After chemical or thermal reduction, this interlayer spacing decreases to only 3.6 Å due to nanochannels collapse (Su et al., 2014). This space is not enough for water and also other molecules to permeate between graphene sheets. Thus, the only permeation path is through the structural defects. Nevertheless, the addition of graphene into materials can bring desired benefits of a different mechanism. Graphene in the membrane matrix reduces the mass transfer resistance caused by collisions between vapor molecules and pore walls due to its vapor adsorption/desorption capacity (Gontarek et al., 2019; Woo, Tijing et al., 2016).

Figure 5. The effect of multilevel roughness on hydrophobicity (SEM images taken from Razmjou et al. (2012)). Copyright permission (License number 4903670873694).

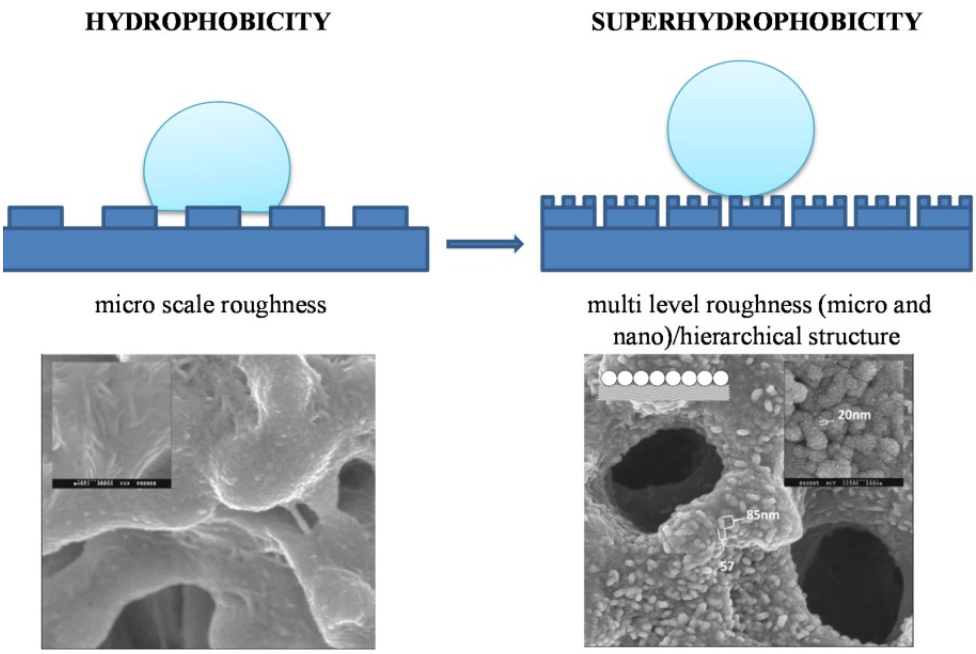

The use of graphene for polymeric membrane modification has been proposed by different researchers. Leaper et al. (2018) prepared mixed-matrix PVDF membranes incorporating GO for AGMD and observed the enhancement of the permeate flux by 52% compared to pure PVDF. Bhadra et al. (2016) prepared GO immobilized PTFE membrane with the enhanced water vapor transport during DCMD. They suggested that multiple factors, such as selective sorption, nanocapillary effect, and reduced temperature polarization affect the improved membrane performance. Nevertheless, the results showed the water droplet on pristine PTFE membrane had a contact angle 110°, while the modification of the polymer with GO resulted in a drop of the angle to 90.6° ± 2.1. This means that GO may reduce the efficiency of MD membranes and is not recommended as an additive for modification of superhydrophobic surfaces. Non-oxidized forms of graphene are a better way to obtain superhydrophobic membrane surfaces. Woo, ~~and~~ Kim et al. (2016) proved the robustness graphene-modified PVDF membrane with improved wetting resistance in long-term air gap membrane distillation. Jafari et al. (2018) prepared a nanofibrous membrane modified with graphene quantum dots (GQD). The results showed an increase in liquid entry pressure of water with a slight decrease in water contact angle. Furthermore, compared to neat PVDF nanofibrous membrane, the GQD-modified membranes revealed higher water flux and salt rejection for air gap MD experiments.

4.2.2. Carbon nanotubes

Other emerging inorganic material, like carbon nanotubes (CNTs), have proved the ability to improve the vapor flux in polymeric matrixes compared to conventional MD membranes (Jamed et al., 2019; Lee et al., 2017). CNTs have a nanocylindrical shape of a rolled-up graphene sheet. Besides strong mechanical properties, CNTs are also chemically and thermally resistant. It is especially important for MD application that CNTs based membranes are characterized by excellent hydrophobicity and porosity. CNTs are able to affect the water-membrane interaction and reduce the permeation of liquid water while favoring the transport of water vapor molecules (Dumée et al., 2011; Gethard et al., 2011). These interactions play an important role in membrane performance, especially in permeability and selectivity. CNT-modified membranes have been applied in solvent extraction (Sae-Khow & Mitra, 2010b), pervaporation (Sae-Khow & Mitra, 2010a) and desalination (Gethard et al., 2011), providing superior performance. It is supposed that

water molecules can diffuse through polymer/CNTs mixed matrix membranes (MMMs) following three possible mechanisms; 1) direct diffusion through continuous polymer matrix, 2) diffusion inside the CNTs through the inner wall, and 3) surface diffusion through the outer wall of CNTs (Lee et al., 2014). Additionally, molecular simulations proved that there exist ordered hydrogen bonds between water molecules during molecular flow through inner part of CNTs (Hinds et al., 2004). These bonds together with the weak interactions between water and hydrophobic walls of CNTs might lead to almost frictionless, thus accelerated flow. In addition, deposited layer of CNTs on a hydrophobic support increases conductive heat transfer from the bulk to the membrane surface, thus reduces thermal polarization and increase membrane performance (Tang et al., 2017). However, high cost of CNTs limits their wide commercial applications. Moreover, in the perspective of water treatment, the point of concern should be focused on the health risks due to the liberation of CNTs into the treated water stream and CNTs stability within the matrix that still remain unknown (Roy et al., 2020).

4.2.3. Metal-oxide nanoparticles

Recently, sphere-like nanoparticles, such as TiO_2, SiO_2 and ZnO, have been reported for MD to create nano-roughness on membrane surfaces. This bioinspired surface is supposed to mimic the lotus effect and create water super-repellency (Chen, Guo et al., 2016). Usually, this super-hydrophobization method includes first nanoparticles coating onto the membrane and then the fluorosilanization with low solid/liquid interface energy material (Boo et al., 2016; Ren et al., 2017; Wang et al., 2018). Such modification not only generates the hierarchical morphology but also decreases diameter of membrane pore providing effective solution to alleviate the issue of membrane pore wetting. Recent studies indicated that coating fluorinated TiO_2 or SiO_2 nanoparticles onto the membrane surface could impart the additional local reentrant structure, which resist wetting by both water and low surface tension liquids (Abd Aziz et al., 2020; Lee et al., 2016).

Among sphere-like nanoparticles, TiO_2 offers some advantages. In principle, it is widely known as an abundant, nontoxic and stable semiconductor and its annual world consumption reaches 4.4 million tones. TiO_2 nanoparticles with various morphologies, such as nanoflowers, nanorods and etc., can be prepared through fast and low-cost hydrothermal synthesis (Chen, Guo et al., 2016; Mali et al., 2011). Several works confirmed a successful TiO_2 implementation to achieve rough and hierarchical surface for applications in membrane distillation (Abd Aziz et al., 2020; Razmjou et al., 2012). Nevertheless, this modification requires an additional step in order to reduce the surface energy. In general, fluorosilanization is the most typical modification applied for conversion of hydrophilic TiO_2 nanoparticles to hydrophobic, however, phosphonic acid modification of TiO_2 has been also reported (Kumar et al., 2020).

Similar to TiO_2 silica is hydrophilic material, however, it is possible to prepare superhydrophobic silica nanoparticles via direct synthesis using hexamethyldisiloxane precursor (Yue et al., 2013), or via postmodification using hydrophobic binders, such as tetraethoxysilane or alkoxysilane (Petcu et al., 2017). These methods provide rough nanoparticles with low interfacial energy. Nevertheless, for MD membrane preparation more popular is a two-step modification strategy including creation of hierarchically micro/nano-scaled roughness using silica nanoparticles (SiNPs) followed by surface energy reduction by fluorination (Shao et al., 2019). To avoid the usage of hazardous fluorinated chemical, Liao et al. (2020) proposed one-step colloid electrospinning/electrospraying to construct hierarchical superhydrophobic surfaces by incorporating silica fumes in the dope solutions. The deposition of modified SiNPs can tune the morphology of various surfaces into superhydrophobic through the formation of a dual-scale roughness layer (Jia et al., 2013). Moreover, modification of silica nanoparticles using hydrophobic molecules enhances their dispersity in polymeric matrixes and organic solvents (Li et al., 2006). On the other hand, it was observed that the incorporation of SiNPs as nanofillers into the membrane weakens the mechanical strength,

therefore, they are usually used together with reinforcement additives such as MWCNTs. Zhou et al. (2019) studied the effect of integrated MWCNTs and SiO_2 on the morphology and performance of the PVDF membrane. When the amount of SiO_2 was relatively low, the vapor flux increased as a result of the synergistic effects between the two filling materials. One of these effects provided by MWCNTs is the increase of overall porosity, while SiO_2 causes the growth of the macrovoids. However, the effect brought by MWCNTs was more dominant. On the other hand, increasing the amount of SiO_2 led to the disappearance of asymmetric structure and low mechanical strength.

Useful properties and rich variety of nanostructures made ZnO well-known for several practical applications, such as optoelectronics, sensors, transducers and biomedical sciences (Wang, 2004). It can be synthesized from readily available raw materials, using low-cost and scalable chemical (Kołodziejczak-Radzimska & Jesionowski, 2014). ZnO nanoparticles are considered to be a promising nanofiller due to their desirable shape, high surface-to-volume ratio, stability under high temperatures and harsh operational conditions and stronger antibacterial property than SiO_2 and TiO_2 (Adams et al., 2006; Anitha et al., 2013; Suresh et al., 2018). Membrane functionalized with ZnO nanoparticles exhibit a rough hierarchical morphology, high contact angle values and low solid/liquid interface energy (Deka et al., 2019). Additionally, ZnO nanoparticles were found to be more economical than other nanoparticles such as TiO_2, and Al_2O_3 (Liang et al., 2012). In the case of alumina, it already gained a huge interest for modification of MF and UF membranes (Gu et al., 2020; Yan et al., 2006; Zhu, Liu, Guan et al., 2019a), however, there are only a few works describing the effect of Al_2O_3 nanoparticles on polymeric membranes for desalination through MD. Although, it was shown recently that it is possible to achieve superhydrophobic surfaces and enhanced PVDF nanofibrous membrane performance using alumina nanoparticles (Attia et al., 2017), the addition of Al_2O_3 has been mainly explored for ceramic MD membranes (Fang et al., 2012; García-Fernández et al., 2017; Subramanian et al., 2019).

4.2.4. Clays

Less popular are clay-based nanocomposites. Although the clay nanocomposites have already found an application in gas separation process (Villaluenga et al., 2007; Xu et al., 2006), there are only a few papers in which clay was used to modify MD membranes. Clays are minerals consist of anionic layered silicates and metal cations, such as Na^+, K^+, Ca^{2+}. The presence of hydrated ions makes them hydrophilic, however, using surfactants through organic cations exchange process, their surface can be easily transformed into hydrophobic (Naderi-Samani et al., 2017). Generally, the addition of clay nanofiller enhances the thermal and surface properties of nanocomposites. The researchers have found out that PVDF-clay hollow fiber membranes showed an increased hydrophobicity and membrane performance during MD testing (Bonyadi & Chung, 2007) than pristine membranes. In another work, nanocomposite nanofiber membranes based on PVDF and clay showed an improved performance in DCMD process and better membrane wetting prevention with the increasing concentration of clay particles (Prince et al., 2012).

4.2.5. Zeolitic imidazolate frameworks

Zeolitic imidazolate frameworks (ZIFs) represent a new class of porous nanostructures. They are a special subclass of metal-organic frameworks (MOFs) with a 3D tetrahedral framework in which metal cations are linked with imidazolate anions. The zeolites framework consists of many cavities and channels (Chen et al., 2014 Chen et al., 2014; Lai, 2018) that make it a potential sorbent material. AQ3 Due to the physical and chemical properties such as high adsorption capacity, ion exchange property and high thermal and chemical stability, ZIFs can be useful for membrane modification. Kebria et al. (2019) prepared a membrane with ultrathin ZIF/chitosan layer on the PVDF surface for AGMD process. Although no significant change in water contact angle was observed, the LEP value increased significantly from 2.2 up to 3.1 bar and the permeate water flux increased about 350% for modified membrane. Li et al. (2020) formed porous hydrophobic ZIF/PVDF layer on the outer surface of PVDF hollow fiber

support membrane in order to further improve the hydrophobicity of the membrane and thus provide special adsorption capacity to the coating layer. In the work conducted by Salehi et al. (2018), the ZIF nanoparticles have been modified in order to increase their hydrophobicity. They have used modified ZnO nanoparticles and silane coupling agent to make the core-shell structure of MZnO@ZIF-8. They observed that the presence of ZIF in membrane increased its porosity, hydrophobicity, permeate flux and rejection.

4.2.6. Dispersion, agglomeration and toxicity of nanomaterials

During the fabrication of nanocomposite membranes, one of the commonly occurring phenomena is nanoparticle aggregation and agglomeration. The nanomaterial concentration can be critical to optimize the performance and durability of nanocomposite membranes. The susceptibility of nanomaterials to aggregate increases when their concentration increases in polymer matrix. This phenomenon often led to a drop-in porosity value and vapor flux reduction (Kumar et al., 2020). For instance, Woo, Tijing et al. (2016) stated that the increase in graphene concentrations in dope solution caused aggregation issues. They observed a decrease in porosity from 94.7% for neat PcH to 82.3% for electrospun membrane with 10 wt% graphene loading. Moreover, it has been proved that the agglomerates result in diminished mechanical strength of nanocomposite. Few strategies have been proposed for improved dispersion of nanofillers including mechanical dispersion, ultrasonication, stirring, chemical modification and physical method (Ma et al., 2010). An et al. (2017) proposed chemical functionalization of CNTs. Non-modified CNTs showed strong agglomeration in entangled bundles. Surface fluorosilanization using FTES led to the significant reduction of agglomeration, improved stability of CNTs and to the fabrication of a well-dispersed membrane. Li et al. (2015) performed the hydrophobization of SiO_2 NPs using OTS in order to improve their dispersion in the PVDF matrix and avoid the nanoparticles agglomeration. Liao, Wang et al. (2014~~a~~) grafted perfluoropolyether (Fluorolink S10) onto the silica surface to assure the homogeneity of dope solution during electrospinning. Unfortunately, most of fluorine compounds exhibit poor degradability in the environment, moreover, they are easily accumulating in living organisms, what may lead to long-term harm. Thus, the evaluation of the potential use of chemicals with lower toxicity should be considered.

Nanomaterials are being increasingly applied in many fields of science. Thus, some of them are inevitably released to the environment, which may bring some harmful effects. For instance, the increase of the concentration of TiO_2 NPs, affects plant growth parameters (Movafeghi et al., 2018), high concentrations of ZnO NPs may reduce the seedlings growth, (Singh et al., 2018) and CNTs affect the oxidation behavior of enzymes in water molecules, which produce toxicity to microorganisms (Chen, Qin et al., 2016). In the case of unmodified graphene, GO and rGO, the majority of current literature agree that they are cytotoxic and genotoxic. Surface modified graphene materials are often less toxic, however, the dose is one of the most important toxicity factor (Guo & Mei~~et al.~~, 2014). On the other hand, the presence of nanomaterials can bring a positive effect on environment remediation, such as organic pollutants and heavy metal absorption (Zhu, Liu, Hu et al., 2019~~b~~).

As a preliminary conclusion of this section, we can notice that specific emerging nano-sized materials are releasing interesting properties to the pristine polymer membranes to reach featured morphological properties for MD separations. The next section addresses the relevant advances in tailoring superhydrophobic membranes and their performance for water desalination.

5. Advances in superhydrophobic membranes improving MD performance

In general, the addition of nanoparticles for polymeric MD membrane preparation can bring excellent water repellency together with a hierarchical and rough structure, and large effective surface area, thereby enhancing the membrane's anti-wetting properties. This can prevent salt deposition, as depicted in the Figure ~~6~~7. Additionally, in case of MMMs,

superhydrophobic inorganic additives can reduce the boundary-layer effect, thus accelerate diffusion in the membrane pores (for example, through an adsorption/desorption assisted diffusion). Such a phenomenon may bring different effects on membrane performance. Herein, the following subsectionss describe in detail the influence of these superhydrophobic pore walls and surface on membrane performance and have been divided into: *i)* stable performance, *ii)* flux enhancement and *iii)* permeate quality. For instance, Table 3 enlists the most relevant development works in preparing superhydrophobic membranes, and their performance in desalination applications.

Figure 6. Scheme of the possible permeation route of water molecules through GO and rGO layers.

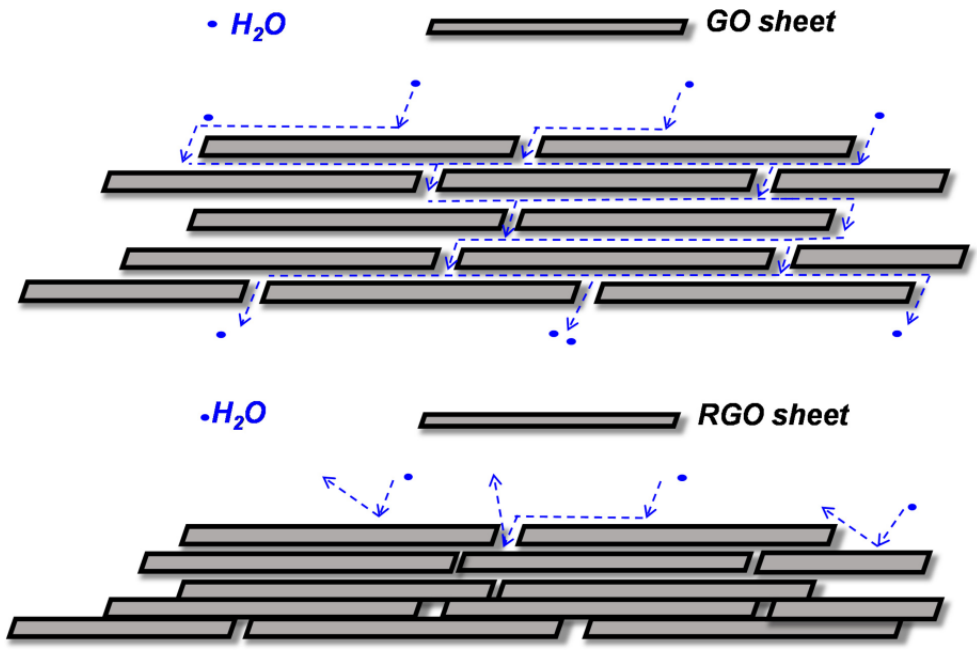

Table 3. Relevant development works in preparing superhydrophobic membranes for desalination.

MD configuration and process parameters	Membrane type	Nanomaterial concentration/nanomaterial layer thickness	Contact angle	LEP	Operating time	Flux/rejection	References
DCMD 3.5 wt.% NaCl Tf: 70 °C Tp: 25 °C	TiO_2 coated PVDF followed by fluorosilanization	no data	163° ± 3°	190 kPa	8 h	□ 30 kg/m² h	Razmjou et al. (2012)
DCMD 3.5 wt.% NaCl Tf: 60 °C Tp:20 °C	PVDF-SiO_2 on PVDF nanofibrous support PVDF-SiO_2 on nonwoven support	6 – 10 wt%/– 8 – 10 wt%/–	>150°	150 kPa 50 kPa	25 h	24.6 ± 1.2 kg/m² h >99.99% 20.8 ± 2.8 kg/m² h >99.99%	Liao, Loh et al. (2014b)

MD configuration and process parameters	Membrane type	Nanomaterial concentration/nanomaterial layer thickness	Contact angle	LEP	Operating time	Flux/rejection	References
DCMD 3.5 wt% NaCl Tf: 60 °C Tp: 20 °C	PVDF-PDA-Ag-thiol nanofiber integrally-modified PVDF-PDA-Ag-thiol nanofiber surface-modified	1 wt%/–	153° ± 4° 158° ± 3°	146 ± 12 kPa 86 ± 22 kPa	8 h	31.6 kg/m^2 h 5.4 kg/m^2 h	Liao, Wang & Fane et al. (2013b)
VMD 200 g/L NaCl Tf: 60 °C ΔP: 80 kPa	ZnO nanorods modified PVDF	–/□2 μm	152°	277 ± 8 kPa	8h	4.5 kg/m^{2}h □99.99%	Wang et al. (2018)
DCMD 3.5 wt.% NaCl Tf: 70 °C Tp: 20 °C DCMD 25 wt.% NaCl Tf: 70 °C Tp: 20 °C	SiO_2 nanoparticles spray-deposited on PVDF	0.2 – 1.5 wt%/–	156°	275 kPa	15 h 180 h	□8 kg/m^2 h 99.99% □5.5 – 4.5 kg/m^2 h 99.99%	Zhang et al. (2013)
VMD 15 wt% NaCl + 6 wt% $MgCl_2$ Tf: 80 °C ΔP: 0.096 MPa	SiO_2 coated PP followed by fluorination	0 – 2.4 wt%/–	150°	–	12 h	□4.5 kg/m^2 h	Shao et al. (2019)
DCMD 3.5 wt.% NaCl Tf: 80 °C Tp: 17 ± 2 °C	electrospun PVDF-clay nanocomposite	0 – 8 wt%/–	154.2° ± 3.0°	200 ± 6 kPa	8 h	□5.75 kg/m^2 h >99.9%	Prince et al. (2012)
DCMD 0.6 M NaCl Tf: 38–56 °C Tp: 15 °C	PVDF/graphene composite	0–10 wt%/–	151° ± 3°	100 kPa	18 h	□9 kg/m^2 h 99.97 – 99.99%	Gontarek et al. (2019)
DCMD 70 g/L NaCl Tf: 60 ± 1 °C Tp: 20 ± 1 °C	CNT-incorporated PcH	1–5 wt%/–	158.5° ± 1.5°	99 kPa	5 h	29.5 kg/m^2 h >99.99%	Tijing et al. (2016)
DCMD 35 g/L NaCl Tf: 60 °C Tp: 20 °C	CNT-PVDF-HFP	0–2 wt%/–	150.4° ± 0.8°	40.5 ± 2.8 kPa	6 h	48.1 kg/m^2 h >99.98%	An et al. (2017)
DCMD 3.5 wt% NaCl Tf: 60 °C Tp: 20 °C	PVDF-SiO_2	10 wt%/–	153.9°	179 kPa	50 h	18.9 kg/m^2 h	Liao, Wang et al. (2014a)
DCMD 3.5 wt% NaCl Tf: 60 °C Tp: 20 °C	PVDF/SiO_2 composite	□6.5 wt%/–	155.6°	230 kPa	24 h	41.1 kg/m^2 h >99.99%	Li et al. (2015)

MD configuration and process parameters	Membrane type	Nanomaterial concentration/nanomaterial layer thickness	Contact angle	LEP	Operating time	Flux/rejection	References
AGMD 3.5 wt% NaCl Tf: 60 °C Tp: 20 °C	PcH/graphene	0.1–2 wt%/–	>162°	>186 kPa	60 h	22.9 kg/m^2 h 100%	Woo, Tijing et al. (2016)
DCMD 30 × 10^3 mgL^{-1} NaCl Tf: 60 °C Tp: 20 °C	SiO_2 embedded PVDF	1 wt%/–	>150°	84.2 ± 2.8 kPa	50 h	34.2 kg/m^2 h >99.9%	Nthunya, Gutierrez, Verliefde et al. (2019b)
DCMD 3.5 wt% NaCl Tf: 70 °C Tp: 25 °C DCMD RO brine Tf: 70 °C Tp: 25 °C	TiO_2 coated PVDF followed by fluorination	–/3 μm	157.1°	158 kPa	10 h 21 h	73.4 kg/m^2 h 99.99% 40.5 kg/m^2 h 99.98%	Ren et al. (2017)
VMD 3.5 wt% NaCl Tf: 50 °C ΔP: 31.3 kPa	ZIFs-incorporated PVDF	0–2 wt%/–	136.5°	215 kPa	60 h	27.1 kg/m^2 h 99.9%	Li et al. (2020)
DCMD 5 g/L NaCl + 0.4 mM SDS ΔT: 53 °C	FAS grafted PVDF withCNTintermediate layer	0.2 wt%/ca.15 μm	180°	–	8 h	28.46 kg/m^2 h –	Wang et al. (2020)

Note. AGMD: air gap membrane distillation, CNT: carbon nanotube, GO: graphene oxide, HFP: hexafluoropropylene, LEP: liquid entry, pressure, LMH: (l/m^{2}h), PcH: Polyvinylidene fluoride-co-hexafluoropropylene, PDA: poly-dopamine, PP: polypropylene, PTFE: polytetrafluoroethylene, PVDF: poly (vinylidene fluoride), Tf: feed temperature, Tp: permeate temperature, VMD: vacuum membrane distillation, ZIF: zeolitic imidazolate framework.

5.1. Performance stability

The durability of the MD system can be hampered by various processes and phenomena, including fouling, heat transfer and concentration polarization. The deposition of foulants can cause the reduction of the flow rate through the membrane in two possible ways, depending on the fouling layer structure, e.g. a homogeneous fouling layer causes pore clogging and reduces the flow rate due to mass transfer resistance, while a porous fouling layer increases susceptibility to temperature polarization effect. Small liquid − solid contact area of a superhydrophobic membrane may effectively reduce the available area for inorganic fouling deposition on the membrane surface (Horseman et al., 2021). Successes in fouling control and wetting mitigation during MD have been observed after membrane coating or modification with nanoparticles. Chen et al. (2018) deposited ZnO nanoparticles on a hydrophilic glass fiber membrane via chemical bath deposition method followed by the surface fluorination and the addition of a polymer coating. The SEM images showed that the ZnO nanoparticles created hierarchical structures on the glass fiber membrane, resulting in water contact angle increase up to 152.8°.The stable water flux was maintained up to 8 h for the low surface tension feed solution. Liao, Wang & Fane et al. (2013b) have prepared integrally-modified and surface-modified PVDF membranes via electrospinning and surface modification. Such membrane preparation protocols involved three steps: the coating nanofiber membrane with poly-dopamine (membrane activation), the coating of the activated surface with silver nanoparticles (morphology and roughness modification), and finally the modification of the surface chemistry with 1-dodecanethiol. Compared with the surface-modified PVDF membranes,

integrally-modified PVDF membranes have been firstly wetted ensuring the introduction of the reagents inside the membrane structure and modification throughout the membrane pores. Interestingly, the proposed method was found to be a simple and effective way to fabricate superhydrophobic nanofiber polymeric membranes. The authors also compared the membrane performance in DCMD process with the unmodified membrane. As both were characterized by a similar pore size distribution, the reason of stable performance in DCMD process for integrally-modified PVDF was its surface properties. Afterwards, the same authors prepared a nature-inspired membrane with a lotus leaf structure. The membrane consisted of scaffold-like PVDF support and a silica-PVDF composite superhydrophobic selective layer made by electrospinning. The membrane exhibited great durability in a continuous DCMD test. Stable performance was observed over 50 h of tests, with the flux of 18.9 kg/m^2 h, while the PVDF nanofiber membrane without a superhydrophobic selective layer displayed only 12.3 kg/m^2 h, the enhanced stability was totally attributed to better surface water repellency.

Zhang et al. (2013) fabricated a superhydrophobic surface by spray-deposition of SiO_2 nanoparticles and PDMS mixture on PVDF membrane. They observed an irregular adhesion of SiO_2 nanoparticles on PVDF surface which contributed to roughness increase. As prepared membranes were characterized with a water contact angle of 156°, and higher LEP value compared to the nonmodified PVDF membranes, which increased from 210 up to 275kPa. In the case of this modification, the flux decreased as a function of the silica content in deposited layer, in other words, the additional layer on the membrane surface caused an increase in its resistance to mass transfer. However, the permeate conductivity of spray-deposited membrane during MD test was constant in the range of 30–50 μS, while in the case of the nonmodified membrane a sharp increase of conductivity can be observed, proving partial wetting of the membrane. It is worth to point out that the modified membrane exhibited better durability and stability during 180 h of operation for high salinity solution with the final NaCl rejection above 99.99%.

Similar to Zhang's study, Li et al. (2015) also used silica nanoparticles to prepare PVDF organic/inorganic composite nanofibrous membranes, which have been found to display an excellent superhydrophobic property together with high LEP of water, resulting in good waterproofness. According to SEM images, the morphology of the membrane contained microwrinkles and nanoprotrusions creating a hierarchical roughness. The modification brought an important improvement to the stability during long-term MD process (over 24 h operating time). Using electrospun PVDF/silica, authors achieved the vapor flux of 41.1kg/m^2 h, and low permeate conductivity (□2.45 μS/cm). Furthermore, no membrane wetting was detected.

Similar results have been found for superhydrophobic membrane obtained by electrospinning of PVDF-clay nanocomposites, which were able to demonstrate a water contact angle up to 154.2°. It has been noted that the contact angle value increased with the clay concentration increase in the membrane. In case of the superhydrophobic membrane with the highest clay concentration of 8 wt.%, no flux decline was observed up to 8 h of operating time. However, the flux of electrospun PVDF–clay presented during DCMD was quite low (□5.5kg/m^{2}h) compared to other membranes used for this application (Prince et al., 2012).

Razmjou et al. (2012) prepared superhydrophobic membranes through the modification of PVDF membranes with TiO_2 coating, which was followed by the surface fluorosilanization. The enhancement of surface hydrophobicity was correlated with the increase of surface roughness together with the reduction in liquid/surface interfacial energy. As a result, the water contact angle ranged from 125° ± 1° for non-modified PVDF up to 163° ± 3° for TiO_2 coated and fluorosilanizated membranes. Moreover, the resulting membranes were characterized with good mechanical and thermal stability. Although no significant enhancement in vapor flux and antifouling properties was observed, there was an important improvement in LEP value for the modified membrane from 120 to 190 kPa. The effect of the LEP

value on the membrane properties was investigated during MD process using 3.5 wt.% sodium chloride solution, where a significant increase in permeate conductivity was observed for the pristine PVDF membrane in comparison with the modified PVDF due to the partial pores wetting.

Incorporation of nanomaterials can also bring a simple way for membrane regeneration during real seawater desalination by membrane distillation. For instance, Guo et al. (2019) fabricated nanofiber ~~poly (vinylidene fluoride-co-hexa-fluoropropene)~~PcH membranes coated with TiO_2 nanoparticles and assessed their performance in 5-day long-term test. Coupled with a ferrate pretreatment followed by dissolved air floatation, MD achieved an improved fouling control. After 5–10 days of MD operation, the water contact angle of the TiO_2 modified membrane was still recoverable up to 150.2° after 30 mins of simple water flushing.

Recently, slippery surface attracts more attention in mitigating the scaling and fouling phenomena in MD (Su et al., 2019). According to Xiao et al. (2019) "slippery surface" refers to the membrane with surface ability to prevent scaling. They introduced the definition of a "stick" or "slippery" surface based on its sliding angle. A "sticky" surface with high sliding angle above 90° might cause non-slip of the liquid phase at the surface. In contrary, the "slippery" surface with low sliding angle exhibits anti-scaling behavior because the liquid remains floating above the polymer phase which arises from very limited interaction of the liquid and the membrane surface. Wang et al. (2020) performed a robust superhydrophobization process by incorporating CNT intermediate layer over commercial PVDF membrane followed with grafting the FAS. As a result, they achieved a~~the~~ superhydrophobic surface with water contact angle of 180° and the water sliding angle of $1-5°$ indicating slippery surface property. Interestingly, a constant flux of 28.46 ± 0.37 kg/m^{2}h and a superior wetting resistance against 0.4 mM SDS w~~as~~ere obtained in DCMD tests as the benefit of constructing the CNT intermediate layer. Superhydrophobic membranes with slippery property were found to reduce the extent of 8 water vapor flux decline caused by gypsum scaling. Yin et al. (2020) formed the superhydrophobic surface through the incorporation of materials with ultra-low surface energy (17-FAS) and a hierarchical texture through grafting of two layers of SiNPs on the PVDF membrane surface. Authors noticed that the incorporation of two different sizes of nanoparticles (120 nm and 30 nm) enhanced the movement of water droplet on the membrane surface, resulting in a slippery property. The superhydrophobic PVDF-Si-FAS membrane with a slippery surface postponed the induction of water flux decline due to gypsum scaling by □100 min compared to pristine PVDF membrane. Similar mitigating effect of membrane with an engineered "slippery" surface on gypsum scaling was reported by Karanikola et al. (2018).

The stability of the coating nanomaterial layers plays an important role in maintaining the membrane performance. However, during MD applications (especially DCMD), membranes are often exposed to high temperatures and cross-flow streams of feed and permeate which could cause the lost of attached nanoparticles. Although not all authors discuss the stability of the nanomaterials in the polymer matrix, performance stability during MD operation may be its determinant. For instance, we can observe a stable vapor flux, for superhydrophobic membranes with hierarchical surface prepared through nanoparticles deposition. As long as we observe a constant vapor flux, we can conclude that the nanomaterials remain on the membrane, simultaneously maintaining its surface properties and structure. Abd Aziz et al. (2020) tested stability of TiO_2 micro/nanoparticles on the membranes surface. They did not observed any significant changes of contact angle after immersing membranes in NaCl solution over ~~for~~ 10 days, which indicates high chemical stability of the coating. Razmjou et al. (2012) analyzed the thermal stability of the TiO_2 coated PVDF membranes by immersing the membrane in hot water (90 °C) for 15 min. They observed a marginal decrease of the contact angle of membrane after the exposure, however, it still remained in the superhydrophobic range. For mixed matrix membranes, physical entrapment can maintain stability of the nanomaterial in the polymer matrix. Tijing et al. (2016) assured that CNTs will not wear off from the membrane structure as a portion of the CNTs is well encapsulated in the polymeric nanofibers. Very recently, Gontarek et al. (2019) collected a vibrational spectra of

filtered residues from feed and permeate streams at the end of MD operation using graphene entrapped membrane. The results indicated no graphene leaking from membranes. Even though these results appear to be promising, most researchers cannot guarantee the stability of the membranes in long-term MD operation as their tests last for a very short duration.

5.2. Flux enhancement

The enhancement of the vapor flux due to the increase in membrane hydrophobicity has been already observed in MD (Dumée et al., 2011; Martínez et al., 2003). There are two possibilities to increase the vapor flux through the membrane, *i)* to increase its driving force, or *ii)* to reduce resistance to mass transport. The increase of the driving force consists of increasing the difference in vapor pressure between both membrane sides, which can be achieved by increasing the temperature difference between feed and permeate, or increasing the effective evaporation area on the feed side. As mentioned previously, an increase in hydrophobicity can prevent the water from penetrating the membrane pores. While the tendency of the pores flooding is minimized, the available vapor exchange surface increases, thus leading to higher vapor flux.

Liao, Loh et al. (2014~~b~~) have proposed two different methods for superhydrophobic membrane preparation via electrospinning. In the first approach, a 3 D superhydrophobic PVDF-silica ultrathin skin was electrospun on nanofibrous PVDF support. Second approach comprised the electrospinning of the thicker layer of 3D superhydrophobic PVDF-silica onto commercial nonwoven support. The superhydrophobic nature of the membrane was confirmed using contact angle measurements, revealing value greater than 150°. The authors proved that the prepared membranes with larger pore size can be potentially used in MD process due to the surface high hydrophobicity. As it turns out, both types of modifications bring valuable improvements to the membrane performance. In the case of nanofiber supported membrane, the enhanced flux can be attributed to the higher porosity, while nonwoven supported membrane was characterized by better mechanical durability for continuous MD operations due to its thicker 3 D structure. Silica nanoparticles were used by Li et al. (2015) and Liao, Wang et al. (2014~~a~~) to prepare superhydrophobic organic/inorganic nanofibrous membranes. These membranes, besides stable performance, were also characterized by increased flux when compared to commercial unmodified membranes. Liao, Wang et al. (2014~~a~~) also noticed strong water repellency of the surface, which was achieved using silica nanoparticles that prevented the membrane from water droplets. The superhydrophobic composite PVDF membrane offered higher effective liquid evaporation area than PVDF nanofiber membrane (see Figure ~~7~~8). Hierarchical rough structures provided numerous holes and slots, which reduce the contact area between solid and liquid, and at the same time increase liquid/vapor contact area. This type of structure promotes water vapor evaporation, and thus increases the permeation flux. In consequence, they have observed flux enhancement from 12.3 kg/m^{2}h for PVDF nanofiber membrane, up to 18.9 kg/m^{2}h for silica/PVDF composite membranes. Importantly, such permeation rates make these membranes highly competitive when compared to commercial flat-sheet PVDF membranes (vapor flux around 10 kg/m^{2}h). Li et al. (2020) observed an increased vapor flux through ZIFs-PVDF hollow fiber composite membrane up to 27.1 kg/m^{2}h. They found that their results could be attributed to four positive effects that emerged with the modification of the membranes. First of all, the formation of ZIF/PVDF layer contributed to the enhancement of membrane roughness and surface water contact angle from 94.5 to 136.5°. Moreover, low thermal conductivity and strong vapor adsorption characteristics of ZIFs effectively accelerate the mass transfer through the membrane, additionally weaken the temperature polarization.

Figure 7. The effect of superhydrophobic additives on MD membrane.

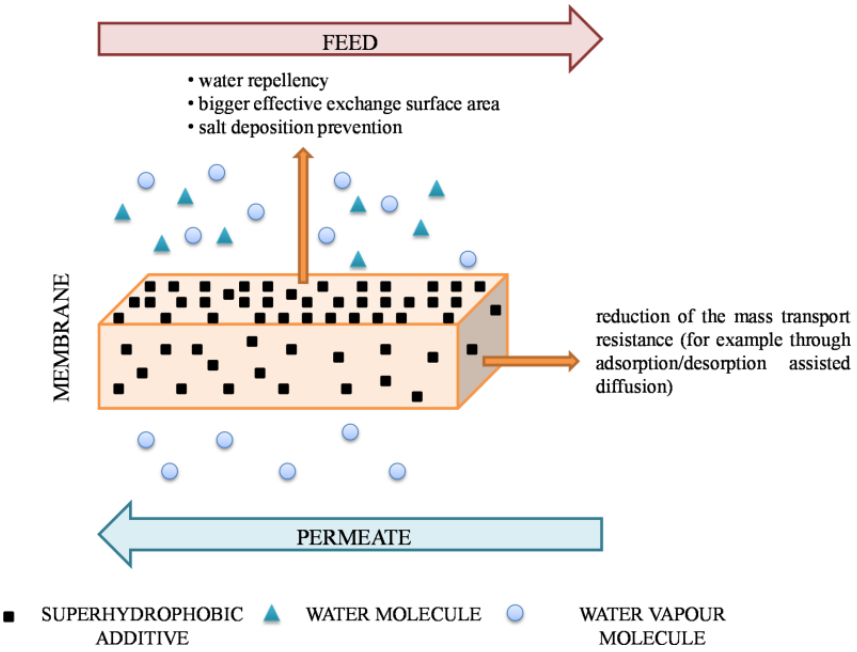

Theoretically, the overall resistance to mass transfer is given by the reciprocal of mass transfer coefficient (k), as follows:

$$\frac{1}{k} = \frac{1}{k^L} + \frac{1}{k^M} + \frac{1}{k^V} \quad (10)$$

where $1/k^L$ is the feed boundary layer resistance, $1/k^M$ is membrane resistance and $1/k^L$ is permeate boundary layer resistance (Vane et al., 2001). It is well-known that the feed boundary layer resistance depends on the feed flow rate and feed solution properties, while the permeate boundary layer resistance is recognized as negligible. The resistances to mass transfer through the membranes are coming from both collisions between vapor molecules and pore walls (i.e. Knudsen diffusion model), or the presence of air trapped in membrane pores and collisions between vapor and air molecules (i.e. molecular diffusion). The superhydrophobicity of the pore walls can reduce mass transfer resistance through mitigation of the negative effect of friction between the pore walls and vapor molecules. The mass transfer behavior within the superhydrophobic membrane can be considered as one having less pore wall collisions that facilitate the flow of vapor through the membrane. Additionally, improved vapor flux through, as called assisted diffusion or adsorption/desorption assisted diffusion, results as well form the reduction of the collisions between pore walls and vapor molecules. As shown in Figure 89, an unassisted transport is chaotic, and composed of many collisions that prolong the vapor molecule way from the feed to the permeate side. In the case of assisted diffusion, the adsorption/desorption capacity of pore walls may facilitate the vapor molecule transport.

Figure 8. Schematic illustration depicting the enlargement of effective evaporation area for silica composite PVDF membranes (figure taken from Liao, Wang et al. (2014~~a~~)).

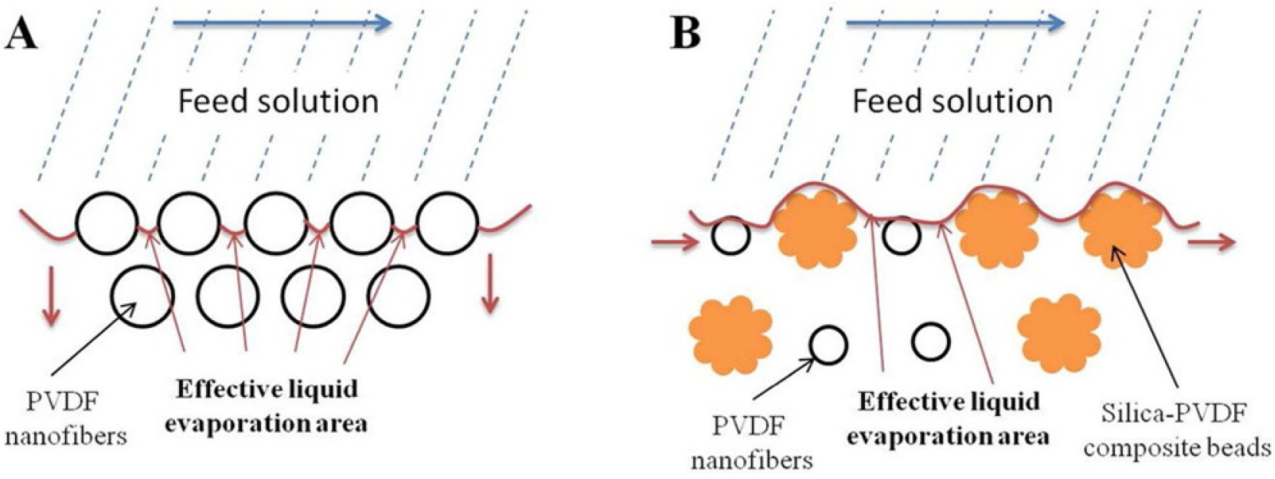

Figure 9. Schematic illustration showing the path of the vapor molecule through the membrane in the case of unassisted and assisted diffusion. AQ19

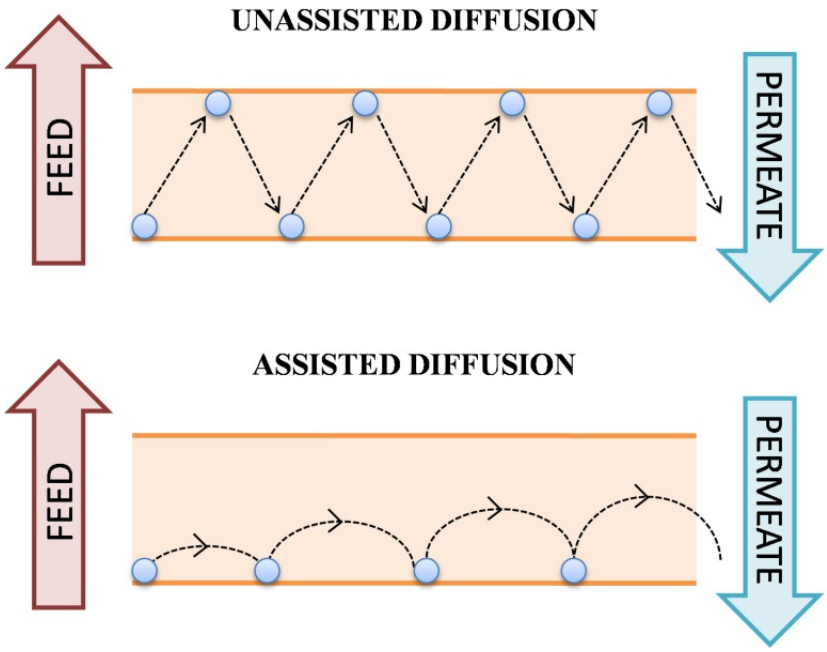

A positive effect of increasing the water vapor flow was seen in membranes modified with CNTs. An et al. (2017) prepared electrospun nanofibres membranes with anchored functionalized CNTs. Due to the covalent modification and fluorination of CNTs, the well dispersibility within the fibers was achieved together with good interfacial interaction between the filler and polymer matrix. Additionally, the authors suggested that the superior mass transfer was a result of the homogeneous embedding of the CNTs. This homogeneity resulted in membrane pore walls superhydrophobicity and effective water vapor molecules repelling, which lead to facilitated Knudsen and molecular diffusion transport and assisted surface diffusion. As a result, they observed around 35% higher average vapor flux value for the CNT modified membrane (□48.1 L/m^{2}h) than that without CNT modification (□33.6 L/m^{2}h). Tijing et al. (2016) prepared mixed matrix ~~polyvinylidene fluoride-co-hexafluoropropylene~~ ~~(~~PcH~~)~~ with different concentrations of CNTs. This particular modification gave the possibility to obtain membranes with comparable pore

size to the commercial PVDF membranes, however, much higher porosity (more than 85%) was reported. Due to the filler incorporation, the surface roughness increased leading to CA increase (of about 158°). The results indicate that CNT-incorporated nanofiber membranes presented 33% and 59% higher fluxes, for 35 and 70 g/L NaCl feed solution in DCMD process, respectively. Herein, the improved membrane performance was explained as an effect of CNTs incorporation. According to authors statement, the modification caused a surface hydrophobicity enhancement, hence, an increase of pore wetting prevention. In general, such changes produced a bigger effective evaporation surface and higher water vapor flux. On the other hand, the presence of CNTs can promote the vapor transport due to its capacity to rapid adsorption/desorption of the vapor molecules (An et al., 2017).

According to Gethard et al. (2011), the rapid adsorption/desorption capacity of CNT allows the vapor molecules to follow a surface diffusion pattern, which increases overall vapor transport. The assisted diffusion may take place along the smooth surface of CNT as well as through their inner tube. They have found the mass transfer coefficient to be higher with the presence of CNTs in the membrane matrix. This increase was especially visible in the range of 60–80 °C, when the mass transfer coefficient was almost 6-fold higher than the unfilled membrane.

In a different approach, an activated diffusion via adsorption/desorption was also observed for electrospun PcH/graphene membranes (Woo, Tijing et al., 2016). The addition of the graphene provoked a vapor flux increase, from 4.75 LMH (L/m^{2}h) for commercial membrane, up to 22.9 LMH for electrospun PcH/graphene membrane. Gontarek et al. (2019) have prepared PVDF/graphene composite membranes, and later tested them in DCMD set-up. The results showed a constant water vapor flux for over 18 h of operating time. Higher values of MD coefficient were observed in the membranes containing low graphene concentration when compared to pristine PVDF membrane. The flux enhancement was noted independently to the porosity decrease of the membranes. In such a study, the mechanism of assisted vapor transport was stated. This increase in water flux was correlated with interactions between graphene filler and water vapor, when the graphene at low concentration was well dispersed over the polymer matrix.

5.3. Permeate quality

The use of saline feed solution in MD may also lead to salt crystallization on the membrane surface and the rise of the partial wetting of the membrane. In theory, the solute molecules can be physically or chemically attached to the membrane surface through interactions with membrane functional groups (Meng et al., 2014). Once the deposition is formed on the membrane surface, the pores can be filled with the feed liquid and consequently, the type of transport is changing (Gryta, 2007). The use of appropriate membrane material may enable the control of partial wetting, thus increasing the permeate quality. According to the literature, a highly hydrophobic membrane can effectively reduce the salt deposition, improve fouling resistance and decrease the possibility of membrane wetting (Razmjou et al., 2012; Wei et al., 2012). Meng et al. (2014) explored the fouling and crystallization behavior of nanocomposite PVDF membranes. They have prepared superhydrophobic surface through TiO_2 and fluorosilane coating, in which the water contact angle increased from $134^{\circ} \pm 0.4$ up to $160^{\circ} \pm 1.4$. These modified membranes showed higher resistance to concentrated salt solutions comparing to pristine membranes. In case of pristine PVDF and PTFE, a fast wetting has occurred due to the close contact with salt crystals that move across the surface, causing local pore enhancement, salt deposition and partial wetting. Due to the superhydrophobic surface modification, the contact between solutes and the membrane decreased as a result of water repulsion. However, not only superhydrophobicity, but also surface structure affects the probability of salt deposition. It was stated that the higher surface roughness decreases the chances of partial membrane wetting and reduces the capability of salt rejection.

Wang et al. (2018) prepared novel ZnO nanorods modified PVDF membrane with a micro/nanoscale hierarchical

structure to solve the membrane fouling and wetting problems. Superhydrophobic surface has been applied to the VMD process for desalination of highly salty water. Modified membrane showed a stable superhydrophobic surface with a contact angle of 152°, easy cleaning property, and unique antifouling and antiwetting properties. After 8 h VMD, the modified membrane showed a similar permeate flux compared to the pristine PVDF membrane but a much higher quality of permeate. The ionic conductivities of the permeate from the pristine PVDF membrane reach 190.88 µS/cm after 8 h, while from the ZnO modified membranes only 10.19 µS/cm. Woc, Tijing et al. (2016) achieved a complete salt rejection (100%) for long-term AGMD by using graphene/PcH membrane, while the commercial membrane displayed around 99.2%. Such results have been attributed to enhanced LEP (>186kPa), contact angle (>162°) and porosity (>88%) values due to the incorporation of graphene and the formation of a multilevel roughness. Shao et al. (2019) modified PP membrane through SiO_2 nanoparticles coating and fluorination for simultaneously enhancement the interface roughness and superhydrophobicity. The membrane was used for highly concentrated saline solution treatment in VMD process. In the case of non-modified PP membranes, the serious membrane fouling in the form of salt crystallization in pores as the water evaporates was observed along with the progressive concentration polarization phenomena. In the contrary, modified membrane presented excellent wetting and fouling resistance during long-term concentration of NaCl and $MgCl_2$ solution. Additionally, no visible crystal embedding in the cross-section was observed. The fouling rate of non-modified membrane increased up to 5.20% for the highest tested feed concentration (15 wt% NaCl, 9 wt% $MgCl_2$) and was four times higher than that of the modified membrane.

In some cases, additional layer of nanomaterials reduces the vapor flux. Nthunya et al. (2020) prepared the superhydrophobic SiO_2-embedded PVDF nanofiber membranes, impregnated with carboxylated multiwalled CNTs and silver nanoparticles to enhance membrane fouling resistance. Although this modification caused a decrease in the initial vapor flux (from 42 LMH to 16 LMH), it also became an effective method for maintaining high salt rejection (recorded rejection decay was from 0.1–1.0%) and stable performance within 50 h of operation. It was observed that, membrane modification reduced the surface cake formation induced by the alginate and biofouling and inhibited the growth of microorganisms.

6. Conclusions and future trends in the field

In this review, an overview of superhydrophobic membranes for MD application is presented, highlighting the mechanisms leading to improved MD performance. This paper also demonstrates that the MMMs and nanoparticles modified membranes attract a lot of attention in superhydrophobic membranes preparation. In general, the recent findings imply the preparation of antiwetting membranes with strong water repellency to improve the membrane stability in long-term MD operation, enhance the vapor flux and improve the permeate quality. Using specific filling materials (such as CNTs, graphene and its derivatives, TiO_2, silica, ZIFs, among others), meaningful desalination performances have been obtained at lab scale. Herein, it is important mentioning that the right selection of the additive may bring multiple benefits and may be the key to obtain membranes for a large-scale processes. However, the emphasis has so far been placed on laboratory-scale experiments. This may be due to the cost of emerging nanofillers, such as graphene and CNTs. At this point, for the new researchers in the field, it is recommended to focus their research interest on cheaper substitutes of these materials but with the same effect on the membrane. Moreover, according to the main drawbacks of MD membranes (e.g. fouling, wetting, stability, heat and mass transfer, resistances), the research should focus their attention on producing next-generation membranes that will be able to meet all of the requirements for real seawater desalination. The formation of hierarchical micro/nano-scale surface morphology (reentrant structure) with air pockets gives the possibility to implement MD for real seawater desalination or industrial wastewater reclamation with the low-surface-tension contaminants (Lu et al., 2019). In addition to high

hydrophobicity and low solid/liquid interface energy, reentrant structure plays an important role in creating omniphobic properties in a membrane, and allows achieving strong repellence toward liquids with a wide range of surface tensions. Thus, omniphobic membranes appear to have promising properties for a real seawater desalination.

Disclosure statement AQ4

No potential conflict of interest was reported by the authors.

References

Note: this Edit/html view does not display references as per your journal style. There is no need to correct this. The content is correct and it will be converted to your journal style in the published version.

Abd Aziz, M. H., Dzarfan Othman, M. H., Alias, N. H., Nakayama, T., Shingaya, Y., Hashim, N. A., Kurniawan, T. A., Matsuura, T., Rahman, M. A., & Jaafar, J. (2020). Enhanced omniphobicity of mullite hollow fiber membrane with organosilane-functionalized TiO2 micro-flowers and nanorods layer deposition for desalination using direct contact membrane distillation. *Journal of Membrane Science*, *607*, 118137. https://doi.org/10.1016/j.memsci.2020.118137

Abraham, J., Vasu, K. S., Williams, C. D., Gopinadhan, K., Su, Y., Cherian, C. T., Dix, J., Prestat, E., Haigh, S. J., Grigorieva, I. V., Carbone, P., Geim, A. K., & Nair, R. R. (2017). Tunable sieving of ions using graphene oxide membranes. *Nature Nanotechnology*, *12*(6), 546–550. https://doi.org/10.1038/nnano.2017.21

Adams, L. K., Lyon, D. Y., & Alvarez, P. J. J. (2006). Comparative eco-toxicity of nanoscale TiO2, SiO2, and ZnO water suspensions. *Water Research*, *40*(19), 3527–3532. https://doi.org/10.1016/j.watres.2006.08.004

Alkhudhiri, A., Darwish, N., & Hilal, N. (2012). Membrane distillation: A comprehensive review. *Desalination*, *287*, 2–18. https://doi.org/10.1016/j.desal.2011.08.027

An, A. K., Lee, E. J., Guo, J., Jeong, S., Lee, J. G., & Ghaffour, N. (2017). Enhanced vapor transport in membrane distillation via functionalized carbon nanotubes anchored into electrospun nanofibres. *Scientific Reports*, *7*, 1–11. https://doi.org/10.1038/srep41562

Anitha, S., Brabu, B., John Thiruvadigal, D., Gopalakrishnan, C., & Natarajan, T. S. (2013). Optical, bactericidal and water repellent properties of electrospun nano-composite membranes of cellulose acetate and ZnO. *Carbohydrate Polymers*, *97*(2), 856–863. https://doi.org/10.1016/j.carbpol.2013.05.003

Attia, H., Alexander, S., Wright, C. J., & Hilal, N. (2017). Superhydrophobic electrospun membrane for heavy metals removal by air gap membrane distillation (AGMD). *Desalination*, *420*, 318–329. https://doi.org/10.1016/j.desal.2017.07.022

Bodell, B. R. (1963). (U.S. Patent No. 3361645). AQ5

Bhadra, M., Roy, S., & Mitra, S. (2014). Nanodiamond immobilized membranes for enhanced desalination via membrane distillation. *Desalination*, *341*(1), 115–119. https://doi.org/10.1016/j.desal.2014.02.036

Bhadra, M., Roy, S., & Mitra, S. (2016). Desalination across a graphene oxide membrane via direct contact membrane distillation. *Desalination*, *378*, 37–43. https://doi.org/10.1016/j.desal.2015.09.026

Bhattarai, S. R., Bhattarai, N., Yi, H. K., Hwang, P. H., Cha, D., & Kim, H. Y. (2004). Novel biodegradable electrospun membrane: Scaffold for tissue engineering. *Biomaterials*, *25*(13) , 2595–2602. https://doi.org/10.1016/j.biomaterials.2003.09.043

Bonyadi, S., & Chung, T. S. (2007). Flux enhancement in membrane distillation by fabrication of dual layer hydrophilic-hydrophobic hollow fiber membranes. *Journal of Membrane Science*, *306*(1–2) , 134–146. https://doi.org/10.1016/j.memsci.2007.08.034

Boo, C., Lee, J., & Elimelech, M. (2016). Engineering surface energy and nanostructure of microporous films for expanded membrane distillation applications. *Environmental Science & Technology*, *50*(15) , 8112–8119. https://doi.org/10.1021/acs.est.6b02316

Cassie, A. B. D., & Baxter, S. (1944). Wettability of porous surfaces. *Transactions of the Faraday Society*, *40*(5), 546–551. https://doi.org/10.1039/tf9444000546

Castro-Muñoz, R., Ahmad, M. Z., & Fíla, V. (2019). Tuning of nano-based materials for embedding into low-permeability polyimides for a featured gas AQ6separation. *Frontiers in Chemistry*, *7*, 897–814. https://doi.org/10.3389/fchem.2019.00897 AQ7

Castro-Muñoz, R., Buera-González, J., Iglesia, Ó. D. L., Galiano, F., Fíla, V., Malankowska, M., Rubio, C., Figoli, A., Téllez, C., & Coronas, J. (2019). Towards the dehydration of ethanol using pervaporation cross-linked poly(vinyl alcohol)/graphene oxide membranes. *Journal of Membrane Science*, *582*, 423–434. https://doi.org/10.1016/j.memsci.2019.03.076

Cerneaux, S., Strużyńska, I., Kujawski, W. M., Persin, M., & Larbot, A. (2009). Comparison of various membrane distillation methods for desalination using hydrophobic ceramic membranes. *Journal of Membrane Science*, *337*(1–2), 55–60. https://doi.org/10.1016/j.memsci.2009.03.025

Chen, B., Yang, Z., Zhu, Y., & Xia, Y. (2014). Zeolitic imidazolate framework materials: recent progress in synthesis and applications. *J. Mater. Chem. A.*, *2*(40), 16811–16831. https://doi.org/10.1039/C4TA02984D

Chen, L., Guo, Z., & Liu, W. (2016). Biomimetic multi-functional superamphiphobic FOTS-TiO2 particles beyond lotus leaf. *ACS Applied Materials & Interfaces*, *8*(40), 27188–27198. https://doi.org/10.1021/acsami.6b06772 AQ8

Chen, L. H., Huang, A., Chen, Y. R., Chen, C. H., Hsu, C. C., Tsai, F. Y., & Tung, K. L. (2018). Omniphobic membranes for direct contact membrane distillation: Effective deposition of zinc oxide nanoparticles. *Desalination*, *428*, 255–263. https://doi.org/10.1016/j.desal.2017.11.029

Chen, M., Qin, X., & Zeng, G. (2016). Single-walled carbon nanotube release affects the microbial enzyme-catalyzed oxidation processes of organic pollutants and lignin model compounds in nature. *Chemosphere*, *163*, 217–226. https://doi.org/10.1016/j.chemosphere.2016.08.031

Cohen-Tanugi, D., & Grossman, J. C. (2012). Water desalination across nanoporous graphene. *Nano Letters*, *12*(7), 3602–3608. https://doi.org/10.1021/nl3012853

Curcio, E., & Drioli, E. (2005). Membrane distillation and related operations - A review. *Separation & Purification Reviews*, *34*(1), 35–86. https://doi.org/10.1081/SPM-200054951

Deka, B. J., Guo, J., Khanzada, N. K., & An, A. K. (2019). Omniphobic re-entrant PVDF membrane with ZnO nanoparticles composite for desalination of low surface tension oily seawater. *Water Research*, *165*, 114982. https://doi.org/10.1016/j.watres.2019.114982

Deshmukh, A., Boo, C., Karanikola, V., Lin, S., Straub, A. P., Tong, T., Warsinger, D. M., & Elimelech, M. (2018). Membrane distillation at the water-energy nexus: Limits, opportunities, and challenges. *Energy & Environmental Science*, *11*(5), 1177–1196. https://doi.org/10.1039/C8EE00291F

Devi, S., Ray, P., Singh, K., & Singh, P. S. (2014). Preparation and characterization of highly micro-porous PVDF membranes for desalination of saline water through vacuum membrane distillation. *Desalination*, *346*, 9–18. https://doi.org/10.1016/j.desal.2014.05.004

Dumée, L., Campbell, J. L., Sears, K., Schütz, J., Finn, N., Duke, M., & Gray, S. (2011). The impact of hydrophobic coating on the performance of carbon nanotube bucky-paper membranes in membrane distillation. *Desalination*, *283*, 64–67. https://doi.org/10.1016/j.desal.2011.02.046

Dumée, L., Germain, V., Sears, K., Schütz, J., Finn, N., Duke, M., Cerneaux, S., Cornu, D., & Gray, S. (2011). Enhanced durability and hydrophobicity of carbon nanotube bucky paper membranes in membrane distillation. *Journal of Membrane Science*, *376*(1–2), 241–246. https://doi.org/10.1016/j.memsci.2011.04.024

Duong, H. C., Chuai, D., Woo, Y. C., Shon, H. K., Nghiem, L. D., & Sencadas, V. (2018). A novel electrospun, hydrophobic, and elastomeric styrene-butadiene-styrene membrane for membrane distillation applications. *Journal of Membrane Science*, *549*, 420–427. https://doi.org/10.1016/j.memsci.2017.12.024

El-Bourawi, M. S., Ding, Z., Ma, R., & Khayet, M. (2006). A framework for better understanding membrane distillation separation process. *Journal of Membrane Science*, *285*(1–2), 4–29. https://doi.org/10.1016/j.memsci.2006.08.002

Eykens, L., De Sitter, K., Dotremont, C., Pinoy, L., & Van der Bruggen, B. (2017). Membrane synthesis for membrane distillation: A review. *Separation and Purification Technology*, *182*, 36–51. https://doi.org/10.1016/j.seppur.2017.03.035

Eykens, L., Hitsov, I., De Sitter, K., Dotremont, C., Pinoy, L., & Van der Bruggen, B. (2017). Direct contact and air gap membrane distillation: Differences and similarities between lab and pilot scale. *Desalination*, *422*, 91–100. https://doi.org/10.1016/j.desal.2017.08.018

Fang, H., Gao, J. F., Wang, H. T., & Chen, C. S. (2012). Hydrophobic porous alumina hollow fiber for water desalination via membrane distillation process. *Journal of Membrane Science*, *403–404*, 41–46. https://doi.org/10.1016/j.memsci.2012.02.011

Findley, M. E. (1967). Vaporization through porous membranes. *Industrial & Engineering Chemistry Process Design and Development*, *6*(2), 226–230. https://doi.org/10.1021/i260022a013

Francis, L., Maab, H., Alsaadi, A., Nunes, S., Ghaffour, N., & Amy, G. L. (2013). Fabrication of electrospun nanofibrous membranes for membrane distillation application. *Desalination and Water Treatment*, *51*(7–9), 1337–1343. https://doi.org/10.1080/19443994.2012.700037

Franken, A. C. M., Nolten, J. A. M., Mulder, M. H. V., Bargeman, D., & Smolders, C. A. (1987). Wetting criteria for the applicability of membrane distillation. *Journal of Membrane Science*, *33*(3), 315–328.

https://doi.org/10.1016/S0376-7388(00)80288-4

García-Fernández, L., Wang, B., García-Payo, M. C., Li, K., & Khayet, M. (2017). Morphological design of alumina hollow fiber membranes for desalination by air gap membrane distillation. *Desalination*, *420*, 226–240. https://doi.org/10.1016/j.desal.2017.07.021

Gethard, K., Sae-Khow, O., & Mitra, S. (2011). Water desalination using carbon-nanotube-enhanced membrane distillation. *ACS Applied Materials & Interfaces*, *3*(2), 110–114. https://doi.org/10.1021/am100981s

Giacomello, A., Meloni, S., Chinappi, M., & Casciola, C. M. (2012). Cassie-Baxter and Wenzel states on a nanostructured surface: Phase diagram, metastabilities, and transition mechanism by atomistic free energy calculations. *Langmuir: The ACS Journal of Surfaces and Colloids*, *28*(29), 10764–10772. https://doi.org/10.1021/la3018453

Goh, S., Zhang, J., Liu, Y., & Fane, A. G. (2013). Fouling and wetting in membrane distillation (MD) and MD-bioreactor (MDBR) for wastewater reclamation *Desalination*, *323*, 39–47. https://doi.org/10.1016/j.desal.2012.12.001

Gontarek, E., Macedonio, F., Militano, F., Giorno, L., Lieder, M., Politano, A., Drioli, E., & Gugliuzza, A. (2019). Adsorption-assisted transport of water vapour in super-hydrophobic membranes filled with multilayer graphene platelets. *Nanoscale*, *11*(24), 11521–11529. https://doi.org/10.1039/c9nr02581b

Gryta, M. (2007). Influence of polypropylene membrane surface porosity on the performance of membrane distillation process. *Journal of Membrane Science*, *287*(1), 67–78. https://doi.org/10.1016/j.memsci.2006.10.011

Gryta, M. (2018). Capillary polypropylene membranes for membrane distillation. *Fibers*, *7*(1), 1–11. https://doi.org/10.3390/fib7010001 AQ9

Gu, Q., Ng, T. C. A., Zhang, L., Lyu, Z., Zhang, Z., Ng, H. Y., & Wang, J. (2020). Interfacial diffusion assisted chemical deposition (ID-CD) for confined surface modification of alumina microfiltration membranes toward high-flux and anti-fouling. *Separation and Purification Technology*, *23*, 116177. https://doi.org/10.1016/j.seppur.2019.116177

Gugliuzza, A., Ricca, F., & Drioli, E. (2006). Controlled pore size, thickness and surface free energy of super-hydrophobic PVDF® and Hyflon®AD membranes *Desalination*, *200*(1–3), 26–28. https://doi.org/10.1016/j.desal.2006.03.229

Guo, J., Deka, B. J., Kim, K. J., & An, A. K. (2019). Regeneration of superhydrophobic TiO2 electrospun membranes in seawater desalination by water flushing in membrane distillation. *Desalination*, *468*, 114054. https://doi.org/10.1016/j.desal.2019.06.020

Guo, X., & Mei, N. (2014). Assessment of the toxic potential of graphene family nanomaterials. *Journal of Food and Drug Analysis*, *22*(1), 105–115. https://doi.org/10.1016/j.jfda.2014.01.009

Han, Y., Xu, Z., & Gao, C. (2013). Ultrathin graphene nanofiltration membrane for water purification. *Advanced Functional Materials*, *23*(29), 3693–3700. https://doi.org/10.1002/adfm.201202601

Hausmann, A., Sanciolo, P., Vasiljevic, T., Weeks, M., Schroën, K., Gray, S., & Duke, M. (2013). Fouling mechanisms of dairy streams during membrane distillation. *Journal of Membrane Science*, *441*, 102–111. https://doi.org/10.1016/j.memsci.2013.03.043

He, F., Gilron, J., Lee, H., Song, L., & Sirkar, K. K. (2008). Potential for scaling by sparingly soluble salts in crossflow DCMD. *Journal of Membrane Science*, *311*(1–2), 68–80. https://doi.org/10.1016/j.memsci.2007.11.056

Himma, N. F., Prasetya, N., Anisah, S., & Wenten, I. G. (2019). Superhydrophobic membrane: Progress in preparation and its separation properties. *Reviews in Chemical Engineering*, *35*(2), 211–238. https://doi.org/10.1515/revce-2017-0030

Hinds, B. J., Chopra, N., Rantell, T., Andrews, R., Gavalas, V., & Bachas, L. G. (2004). Aligned multiwalled carbon nanotube membranes. *Science (New York, N.Y.)*, *303*(5654), 62–65. https://doi.org/10.1126/science.1092048

Horseman, T., Yin, Y., Christie, K. S., Wang, Z., Tong, T., & Lin, S. (2021). Wetting, scaling, and fouling in membrane distillation: State-of-the-art insights on fundamental mechanisms and mitigation strategies. *ACS ES&T Engineering*, *1*(1), 117–140. https://doi.org/10.1021/acsestengg.0c00025 AQ10

Jafari, A., Kebria, M. R. S., Rahimpour, A., & Bakeri, G. (2018). Graphene quantum dots modified polyvinylidenefluride (PVDF) nanofibrous membranes with enhanced performance for air Gap membrane distillation. *Chemical Engineering and Processing - Process Intensification*, *126*(2010), 222–231. https://doi.org/10.1016/j.cep.2018.03.010

Jamed, M. J., Alhathal Alanezi, A., & Alsalhy, Q. F. (2019). Effects of embedding functionalized multi-walled carbon nanotubes and alumina on the direct contact poly(vinylidene fluoride-co-hexafluoropropylene) membrane distillation performance. *Chemical Engineering Communications*, *206*(8), 1035–1057. https://doi.org/10.1080/00986445.2018.1542302

Jeong, S., Shin, B., Jo, W., Kim, H. Y., Moon, M. W., & Lee, S. (2016). Nanostructured PVDF membrane for MD application by an O2and CF4plasma treatment. *Desalination*, *399*, 178–184. https://doi.org/10.1016/j.desal.2016.09.001

Jia, Y., Yue, R., Liu, G., Yang, J., Ni, Y., Wu, X., & Chen, Y. (2013). Facile fabrication of nano-structured silica hybrid film with superhydrophobicity by one-step VAFS approach. *Applied Surface Science*, *265*, 405–411. https://doi.org/10.1016/j.apsusc.2012.11.020

Joshi, R. K., Carbone, P., Wang, F. C., Kravets, V. G., Su, Y., Grigorieva, I. V., Wu, H. A., Geim, A. K., & Nair, R. R. (2014). Precise and ultrafast molecular sieving through graphene oxide membranes. *Science (New York, N.Y.)*, *343*(6172), 752–754. https://doi.org/10.1126/science.1245711

Karanikola, V., Boo, C., Rolf, J., & Elimelech, M. (2018). Engineered slippery surface to mitigate gypsum scaling in membrane distillation for treatment of hypersaline industrial wastewaters. *Environmental Science & Technology*, *52*(24), 14362–14370. https://doi.org/10.1021/acs.est.8b04836

Ke, H., Feldman, E., Guzman, P., Cole, J., Wei, Q., Chu, B., Alkhudhiri, A., Alrasheed, R., & Hsiao, B. S. (2016). Electrospun polystyrene nanofibrous membranes for direct contact membrane distillation. *Journal of Membrane Science*, *515*, 86–97. https://doi.org/10.1016/j.memsci.2016.05.052

Kebria, M. R. S., Rahimpour, A., Bakeri, G., & Abedini, R. (2019). Experimental and theoretical investigation of thin ZIF-8/chitosan coated layer on air gap membrane distillation performance of PVDF membrane. *Desalination*, *450*, 21–32. https://doi.org/10.1016/j.desal.2018.10.023

Khayet, M., Mengual, J . I., & Matsuura, T. (2005) . Porous hydrophobic/hydrophilic composite membranes: Application in desalination using direct contact membrane distillation. *Journal of Membrane Science*, *252*(1–2), 101–113. https://doi.org/10.1016/j.memsci.2004.11.022

Khayet, M., Velázquez, A., & Mengual, J. I. (2004). Modelling mass transport through a porous partition: Effect of pore size distribution. *Journal of Non-Equilibrium Thermodynamics*, *29*(3) , 279–299. https://doi.org/10.1515/JNETDY.2004.055

Kołodziejczak-Radzimska, A., & Jesionowski, T. (2014) . Zinc oxide-from synthesis to application: A review. *Materials (Basel, Switzerland)*, *7*(4), 2833–2881. https://doi.org/10.3390/ma7042833

Kullab, A., & Martin, A. (2011). Membrane distillation and applications for water purification in thermal cogeneration plants. *Separation and Purification Technology*, *76*(3), 231–237. https://doi.org/10.1016/j.seppur.2010.09.028

Kumar, R., Ahmed, M., Bhadrachari, G., Al-Mesri, A., & Thomas, J . P. (2020) . A facile approach of thin film coating consisted of hydrophobic titanium dioxide over polypropylene membrane for membrane distillation graphical abstract keywords. ~~https://doi.org/10.22079/JMSR.2019.110904.1273~~*Journal of Membrane Science and Research*, *6*(2), 196–202. https://doi.org/10.22079/JMSR.2019.110904.1273 **AQ11**

Laganà, F., Barbieri, G., & Drioli, E. (2000) . Direct contact membrane distillation: Modelling and concentration experiments. *Journal of Membrane Science*, *166*(1), 1–11. https://doi.org/10.1016/S0376-7388(99)00234-3

Lai, Z. (2018). Development of ZIF-8 membranes: Opportunities and challenges for commercial applications *Current Opinion in Chemical Engineering*, *20*, 78–85. https://doi.org/10.1016/j.coche.2018.03.002

Larbot, A., Gazagnes, L., Krajewski, S., Bukowska, M., & Kujawski, W. (2004). Water desalination using ceramic membrane distillation. Desalination, *168*, 367–372. **AQ12**

Lawson, K . W., & Lloyd, D . R. (1997) . Membrane distillation. *Journal of Membrane Science*, *124*(1) , 1–25. https://doi.org/10.1007/s00216-011-4733-9

Leaper, S., Abdel-Karim, A., Faki, B., Luque-Alled, J. M., Alberto, M., Vijayaraghavan, A., Holmes, S. M., Szekely, G., Badawy, M. I., Shokri, N., & Gorgojo, P. (2018). Flux-enhanced PVDF mixed matrix membranes incorporating APTS-functionalized graphene oxide for membrane distillation *Journal of Membrane Science*, *554*, 309–323. https://doi.org/10.1016/j.memsci.2018.03.013

Lee, H. D., Kim, H. W., Cho, Y. H., & Park, H. B. (2014). Experimental evidence of rapid water transport through carbon nanotubes embedded in polymeric desalination membranes. *Small (Weinheim an Der Bergstrasse, Germany)*, *10*(13), 2653–2660. https://doi.org/10.1002/smll.201303945

Lee, J., Boo, C., Ryu, W. H., Taylor, A . D., & Elimelech, M. (2016) . Development of omniphobic desalination membranes using a charged electrospun nanofiber scaffold. *ACS Applied Materials & Interfaces*, *8*(17), 11154–11161. https://doi.org/10.1021/acsami.6b02419

Lee, J.-G., Lee, E.-J., Jeong, S., Guo, J., An, A . K., Guo, H., Kim, J., Leiknes, T., & Ghaffour, N. (2017). Theoretical modeling and experimental validation of transport and separation properties of carbon nanotube electrospun membrane distillation. *Journal of Membrane Science*, *526*, 395–408. https://doi.org/10.1016/j.memsci.2016.12.045

Li, H., Liu, H., Shi, W., Zhang, H., Zhou, R., & Qin, X. (2020). Preparation of hydrophobic zeolitic imidazolate framework-71 (ZIF-71)/PVDF hollow fiber composite membrane for membrane distillation through dilute solution coating. *Separation and Purification Technology*, *251*, 117348. https://doi.org/10.1016/j.seppur.2020.117348

Li, X., Cao, Z., Zhang, Z., & Dang, H. (2006). Surface-modification in situ of nano-SiO 2 and its structure and tribological properties. *Applied Surface Science*, *252*(22), 7856–7861. https://doi.org/10.1016/j.apsusc.2005.09.068

Li, X., Yu, X., Cheng, C., Deng, L., Wang, M., & Wang, X. (2015). Electrospun superhydrophobic organic/inorganic composite nanofibrous membranes for membrane distillation. *ACS Applied Materials & Interfaces*, *7*(39), 21919–21930. https://doi.org/10.1021/acsami.5b06509

Li, X. M., Reinhoudt, D., & Crego-Calama, M. (2007). What do we need for a superhydrophobic surface? A review on the recent progress in the preparation of superhydrophobic surfaces. *Chemical Society Reviews*, *36*(8), 1350–1368. https://doi.org/10.1039/b602486f

Liang, S., Xiao, K., Mo, Y., & Huang, X. (2012). A novel ZnO nanoparticle blended polyvinylidene fluoride membrane for anti-irreversible fouling. *Journal of Membrane Science*, *394–395*, 184–192. https://doi.org/10.1016/j.memsci.2011.12.040

Liao, Y., Loh, C. H., Wang, R., & Fane, A. G. (2014). Electrospun superhydrophobic membranes with unique structures for membrane distillation. *ACS Applied Materials & Interfaces*, *6*(18), 16035–16048. https://doi.org/10.1021/am503968n

Liao, Y., Wang, R., & Fane, A. G. (2013). Engineering superhydrophobic surface on poly(vinylidene fluoride) nanofiber membranes for direct contact membrane distillation. *Journal of Membrane Science*, *440*, 77–87. https://doi.org/10.1016/j.memsci.2013.04.006

Liao, Y., Wang, R., & Fane, A. G. (2014). Fabrication of bioinspired composite nanofiber membranes with robust superhydrophobicity for direct contact membrane distillation. *Environmental Science & Technology*, *48*(11), 6335–6341. https://doi.org/10.1021/es405795s

Liao, Y., Wang, R., Tian, M., Qiu, C., & Fane, A. G. (2013). Fabrication of polyvinylidene fluoride (PVDF) nanofiber membranes by electro-spinning for direct contact membrane distillation. *Journal of Membrane Science*, *425–426*, 30–39. https://doi.org/10.1016/j.memsci.2012.09.023

Liao, Y., Zheng, G., Huang, J. J., Tian, M., & Wang, R. (2020). Development of robust and superhydrophobic membranes to mitigate membrane scaling and fouling in membrane distillation. *Journal of Membrane Science*, *601*, 117962. https://doi.org/10.1016/j.memsci.2020.117962

Lu, K. J., Chen, Y., & Chung, T. S. (2019). Design of omniphobic interfaces for membrane distillation - A review. *Water Research*, *162*, 64–77. https://doi.org/10.1016/j.watres.2019.06.056

Ma, M., Hill, R. M., Lowery, J. L., Fridrikh, S. V., & Rutledge, G. C. (2005). Electrospun poly(styrene-block-dimethylsiloxane) block copolymer fibers exhibiting superhydrophobicity. *Langmuir: The ACS Journal of Surfaces and Colloids*, *21*(12), 5549–5554. https://doi.org/10.1021/la047064y

Ma, P. C., Siddiqui, N. A., Marom, G., & Kim, J. K. (2010). Dispersion and functionalization of carbon nanotubes for polymer-based nanocomposites: A review. *Composites Part A: Applied Science and Manufacturing*, *41*(10),

1345–1367. https://doi.org/10.1016/j.compositesa.2010.07.003

Macedonio, F., & Drioli, E. (2008). Pressure-driven membrane operations and membrane distillation technology integration for water purification. *Desalination*, *223*(1–3), 396–409. https://doi.org/10.1016/j.desal.2007.01.200

Mackie, J. S., & Meares, P. (1955). The diffusion of electrolytes in a cation-exchange resin membrane. *Proceedings of Royal Society*, *A232*, 498–509. https://doi.org/10.1246/nikkashi1921.58.819

Mali, S. S., Betty, C. A., Bhosale, P. N., & Patil, P. S. (2011). Hydrothermal synthesis of rutile TiO2 with hierarchical microspheres and their characterization. *CrystEngComm*, *13*(21) , 6349–6351. https://doi.org/10.1039/c1ce05928a

Martínez, L., Florido-Díaz, F. J., Hernández, A., &., & Prádanos, P., (2003). Estimation of vapor transfer coefficient of hydrophobic porous membranes for applications in membrane distillation. *Separation and Purification Technology*, *33*(1), 45–55. https://doi.org/10.1016/S1383-5866(02)00218-6

McHale, G., Shirtcliffe, N. J., & Newton, M. I. (2004). Super-hydrophobic and super-wetting surfaces: Analytical potential? *The Analyst*, *129*(4), 284–287. https://doi.org/10.1039/b400567h

Meng, S., Ye, Y., Mansouri, J., & Chen, V. (2014). Fouling and crystallisation behaviour of superhydrophobic nano-composite PVDF membranes in direct contact membrane distillation *Journal of Membrane Science*, *463*, 102–112. https://doi.org/10.1016/j.memsci.2014.03.027

Movafeghi, A., Khataee, A., Abedi, M., Tarrahi, R., Dadpour, M., & Vafaei, F. (2018). Effects of TiO2 nanoparticles on the aquatic plant Spirodela polyrrhiza: Evaluation of growth parameters, pigment contents and antioxidant enzyme activities. *Journal of Environmental Sciences*, *64*, 130–139. https://doi.org/10.1016/j.jes.2016.12.020 **AQ13**

Naderi-Samani, H., Loghman-Estarki, M. R., Razavi, R. S., & Ramazani, M. (2017). The effects of organoclay on the morphology, thermal stability, transparence and hydrophobicity properties of polyamide − imide/nanoclay nanocomposite coatings. *Progress in Organic Coatings*, *112*, 162–168. https://doi.org/10.1016/j.porgcoat.2017.07.012

Nair, R. R., Wu, H. A., Jayaram, P. N., Grigorieva, I. V., & Geim, A. K. (2012). Unimpeded permeation of water through helium-leak-tight graphene-based membranes. *Science (New York, N.Y.)*, *335*(6067) , 442–444. https://doi.org/10.1126/science.1211694

Nthunya, L. N., Gutierrez, L., Derese, S., Nxumalo, E. N., Verliefde, A. R., Mamba, B. B., & Mhlanga, S. D. (2019). A review of nanoparticle-enhanced membrane distillation membranes: Membrane synthesis and applications in water treatment. *Journal of Chemical Technology & Biotechnology*, *94*(9) , 2757–2771. https://doi.org/10.1002/jctb.5977

Nthunya, L. N., Gutierrez, L., Nxumalo, E. N., Verliefde, A. R., Mhlanga, S. D., & Onyango, M. S. (2020). f-MWCNTs/AgNPs-coated superhydrophobic PVDF nanofibre membrane for organic, colloidal, and biofouling mitigation in direct contact membrane distillation. *Journal of Environmental Chemical Engineering*, *8*(2), 103654. https://doi.org/10.1016/j.jece.2020.103654

Nthunya, L. N., Gutierrez, L., Verliefde, A. R., & Mhlanga, S. D. (2019). Enhanced flux in direct contact membrane distillation using superhydrophobic PVDF nanofibre membranes embedded with organically modified SiO2

nanoparticles. *Journal of Chemical Technology & Biotechnology*, *94*(9) , 2826–2837. https://doi.org/10.1002/jctb.6104

Ogawa, T., Ding, B., Sone, Y., & Shiratori, S. (2007). Super-hydrophobic surfaces of layer-by-layer structured film-coated electrospun nanofibrous membranes. *Nanotechnology*, *18*(16), 165607–165608. https://doi.org/10.1088/0957-4484/18/16/165607

Ollivier, H. (1907). Annales de Chimie et de Physique. *Annales de Chimie et de Physique*, *10*, 229.

Onda, T., Shibuichi, S., Satoh, N., & Tsujii, K. (1996). Super-water-repellent fractal surfaces. Langmuir, *12*(9), 5–7. AQ14

Orfi, J., Loussif, N., & Davies, P. A. (2016). Heat and mass transfer in membrane distillation used for desalination with slip flow. *Desalination*, *381*, 135–142. https://doi.org/10.1016/j.desal.2015.12.009

Pan, C.-Y., Xu, G.-R., Xu, K., Zhao, H.-L., Wu, Y.-Q., Su, H.-C., Xu, J.-M., & Das, R. (2019). Electrospun nanofibrous membranes in membrane distillation: Recent developments and future perspectives. *Separation and Purification Technology*, *221*, 44–63. https://doi.org/10.1016/j.seppur.2019.03.080

Peng, Y., Dong, Y., Fan, H., Chen, P., Li, Z., & Jiang, Q. (2013). Preparation of polysulfone membranes via vapor-induced phase separation and simulation of direct-contact membrane distillation by measuring hydrophobic layer thickness. *Desalination*, *316*, 53–66. https://doi.org/10.1016/j.desal.2013.01.021

Petcu, C., Purcar, V., Spătaru, C.-I., Alexandrescu, E., Şomoghi, R., Trică, B., Niţu, S., Panaitescu, D., Donescu, D., & Jecu, M.-L. (2017). The influence of new hydrophobic silica nanoparticles on the surface properties of the films obtained from bilayer hybrids. *Nanomaterials*, *7*(2), 47–10. https://doi.org/10.3390/nano7020047

Prince, J. A., Singh, G., Rana, D., Matsuura, T., Anbharasi, V., & Shanmugasundaram, T. S. (2012). Preparation and characterization of highly hydrophobic poly(vinylidene fluoride) - Clay nanocomposite nanofiber membranes (PVDF-clay NNMs) for desalination using direct contact membrane distillation. *Journal of Membrane Science*, *397–398*, 80–86. https://doi.org/10.1016/j.memsci.2012.01.012

Razmjou, A., Arifin, E., Dong, G., Mansouri, J., & Chen, V. (2012). Superhydrophobic modification of TiO 2 nanocomposite PVDF membranes for applications in membrane distillation. *Journal of Membrane Science*, *415–416*, 850–863. https://doi.org/10.1016/j.memsci.2012.06.004

Ren, L. F., Xia, F., Chen, V., Shao, J., Chen, R., & He, Y. (2017). TiO2-FTCS modified superhydrophobic PVDF electrospun nanofibrous membrane for desalination by direct contact membrane distillation. *Desalination*, *423*, 1–11. https://doi.org/10.1016/j.desal.2017.09.004

Reneker, D. H., & Yarin, A. L. (2008). Electrospinning jets and polymer nanofibers. *Polymer*, *49*(10), 2387–2425. https://doi.org/10.1016/j.polymer.2008.02.002

Roy, K., Mukherjee, A., Maddela, N. R., Chakraborty, S., Shen, B., Li, M., Du, D., Peng, Y., Lu, F., & García Cruzatty, L. C. (2020). Outlook on the bottleneck of carbon nanotube in desalination and membrane-based water treatment-A review. *Journal of Environmental Chemical Engineering*, *8*(1) , 103572. https://doi.org/10.1016/j.jece.2019.103572

Sae-Khow, O., & Mitra, S. (2010a) . Carbon nanotube immobilized composite hollow fiber membranes for pervaporative removal of volatile organics from water. *The Journal of Physical Chemistry C*, *114*(39), 16351–16356.

https://doi.org/10.1021/jp1064402

Sae-Khow, O., & Mitra, S. (2010b). Simultaneous extraction and concentration in carbon nanotube immobilized hollow fiber membranes. *Analytical Chemistry*, *82*(13), 5561–5567. https://doi.org/10.1021/ac100426y

Salehi, S., Jahanshahi, M., & Peyravi, M. (2018). Poly(vinylidene difluoride) membrane assisted by modified ZnO/ZIF nanoparticles for membrane distillation *Chemical Engineering & Technology*, *41*(10) , 1994–2004. https://doi.org/10.1002/ceat.201700496

Schneider, K., Hölz, W., Wollbeck, R., & Ripperger, S. (1988). Membranes and modules for transmembrane distillation. *Journal of Membrane Science*, *39*(1), 25–42. https://doi.org/10.1016/S0376-7388(00)80992-8

Seyed Shahabadi, S. M., Rabiee, H., Seyedi, S. M., Mokhtare, A., & Brant, J. A. (2017). Superhydrophobic dual layer functionalized titanium dioxide/polyvinylidene fluoride-co-hexafluoropropylene (TiO2/PH) nanofibrous membrane for high flux membrane distillation. *Journal of Membrane Science*, *537*, 140–150. https://doi.org/10.1016/j.memsci.2017.05.039

Shao, Y., Han, M., Wang, Y., Li, G., Xiao, W., Li, X., Wu, X., Ruan, X., Yan, X., He, G., & Jiang, X. (2019). Superhydrophobic polypropylene membrane with fabricated antifouling interface for vacuum membrane distillation treating high concentration sodium/magnesium saline water. *Journal of Membrane Science*, *579*, 240–252. https://doi.org/10.1016/j.memsci.2019.03.007

Shirtcliffe, N. J., McHale, G., Atherton, S., & Newton, M. I. (2010). An introduction to superhydrophobicity. *Advances in Colloid and Interface Science*, *161*(1–2), 124–138. https://doi.org/10.1016/j.cis.2009.11.001

Singh, A., Prasad, S. M., & Singh, S. (2018). Environmental nanotechnology, monitoring & management impact of nano ZnO on metabolic attributes and fl uorescence kinetics of rice seedlings. *Environmental Nanotechnology, Monitoring & Management*, *9*, 42–49. https://doi.org/10.1016/j.enmm.2017.11.006

Smolders, K., & Franken, A. C. M. (1989). Terminology for membrane distillation. *Desalination*, *72*(3), 249–262. https://doi.org/10.1016/0011-9164(89)80010-4

Srisurichan, S., Jiraratananon, R., & Fane, A. G. (2006). Mass transfer mechanisms and transport resistances in direct contact membrane distillation process. *Journal of Membrane Science*, *277*(1–2) , 186–194. https://doi.org/10.1016/j.memsci.2005.10.028

Su, C., Horseman, T., Cao, H., Christie, K. S. S., Li, Y., & Lin, S. (2019). Robust superhydrophobic membrane for membrane distillation with excellent scaling resistance. *Environmental Science and Technology, 53, 11801−11809*. https://doi.org/10.1021/acs.est.9b04362 **AQ15**

Su, Y., Kravets, V. G., Wong, S. L., Waters, J., Geim, A. K., & Nair, R. R. (2014). Impermeable barrier films and protective coatings based on reduced graphene oxide. *Nature Communications*, *5*(1) , 1–5. https://doi.org/10.1038/ncomms5843

Subramanian, N., Qamar, A., Alsaadi, A., Gallo, A., Ridwan, M. G., Lee, J.-G., Pillai, S., Arunachalam, S., Anjum, D., Sharipov, F., Ghaffour, N., & Mishra, H. (2019). Evaluating the potential of superhydrophobic nanoporous alumina membranes for direct contact membrane distillation. *Journal of Colloid and Interface Science*, *533*, 723–732. https://doi.org/10.1016/j.jcis.2018.08.054

Sun, P., Zhu, M., Wang, K., Zhong, M., Wei, J., Wu, D., Xu, Z., & Zhu, H. (2013). Selective ion penetration of graphene oxide membranes. *ACS Nano*, *7*(1), 428–437. https://doi.org/10.1021/nn304471w

Suresh, J., Pradheesh, G., Alexramani, V., Sundrarajan, M., & Hong, S . I. (2018) . Green synthesis and characterization of zinc oxide nanoparticle using insulin plant (Costus pictus D. Don) and investigation of its antimicrobial as well as anticancer activities. *Advances in Natural Sciences: Nanoscience and Nanotechnology*, *9*(1), 1-8. https://doi.org/10.1088/2043-6254/aaa6f1 AQ16

Takashi, N., Masashi, M., Katsuhiko, N., Motonori, M., & Yasukiyo, U. (1999). The lowest surface free energy based on − CF3 alignment. *Langmuir*, *15*(13), 4321–4323. https://doi.org/10.1021/la981727s

Tamura, T., & Kawakami, H. (2010). Aligned electrospun nanofiber composite membranes for fuel cell electrolytes. *Nano Letters*, *10*(4), 1324–1328. https://doi.org/10.1021/nl1007079

Tang, L., Iddya, A., Zhu, X., Dudchenko, A. V., Duan, W., Turchi, C., Vanneste, J., Cath, T. Y., & Jassby, D. (2017) . Enhanced flux and electrochemical cleaning of silicate scaling on carbon nanotube-coated membrane distillation membranes treating geothermal brines. *ACS Applied Materials & Interfaces*, *9*(44) , 38594–38605. https://doi.org/10.1021/acsami.7b12615

Tang, N., Jia, Q., Zhang, H., Li, J., & Cao, S. (2010). Preparation and morphological characterization of narrow pore size distributed polypropylene hydrophobic membranes for vacuum membrane distillation via thermally induced phase separation. *Desalination*, *256*(1–3), 27–36. https://doi.org/10.1016/j.desal.2010.02.024

Termpiyakul, P., Jiraratananon, R., & Srisurichan, S. (2005). Heat and mass transfer characteristics of a direct contact membrane distillation process for desalination. *Desalination*, *177*(1–3) , 133–141. https://doi.org/10.1016/j.desal.2004.11.019

Tian, M., Yin, Y., Yang, C., Zhao, B., Song, J., Liu, J., Li, X.-M., & He, T. (2015). CF4 plasma modified highly interconnective porous polysulfone membranes for direct contact membrane distillation (DCMD) *Desalination*, *369*, 105–114. https://doi.org/10.1016/j.desal.2015.05.002

Tijing, L. D., Woo, Y. C., Shim, W. G., He, T., Choi, J. S., Kim, S. H., & Shon, H. K. (2016). Superhydrophobic nanofiber membrane containing carbon nanotubes for high-performance direct contact membrane distillation. *Journal of Membrane Science*, *502*, 158–170. https://doi.org/10.1016/j.memsci.2015.12.014

Vane, L. M., Alvarez, F. R., & Mullins, B. (2001). Removal of methyl tert-butyl ether from water by pervaporation: Bench- and pilot-scale evaluations. *Environmental Science & Technology*, *35*(2) , 391–397. https://doi.org/10.1021/es001362 +

Villaluenga, J. P. G., Khayet, M., López-Manchado, M. A., Valentin, J. L., Seoane, B., & Mengual, J. I. (2007). Gas transport properties of polypropylene/clay composite membranes. *European Polymer Journal*, *43*(4) , 1132–1143. https://doi.org/10.1016/j.eurpolymj.2007.01.018

Wang, J. W., Li, L., Zhang, J. W., Xu, X., & Chen, C. S. (2016). β-Sialon ceramic hollow fiber membranes with high strength and low thermal conductivity for membrane distillation. *Journal of the European Ceramic Society*, *36*(1), 59–65. https://doi.org/10.1016/j.jeurceramsoc.2015.09.027

Wang, M., Liu, G., Yu, H., Lee, S.-H., Wang, L., Zheng, J., Wang, T., Yun, Y., & Lee, J. K. (2018). ZnO nanorod array modified PVDF membrane with superhydrophobic surface for vacuum membrane distillation application *ACS*

Applied Materials & Interfaces, *10*(16), 13452–13461. https://doi.org/10.1021/acsami.8b00271

Wang, R., Liu, Y., Li, B., Hsiao, B. S., & Chu, B. (2012). Electrospun nanofibrous membranes for high flux microfiltration. *Journal of Membrane Science*, *392–393*, 167–174. https://doi.org/10.1016/j.memsci.2011.12.019

Wang, Y., Han, M., Liu, L., Yao, J., & Han, L. (2020). Beneficial CNT intermediate layer for membrane fluorination toward robust superhydrophobicity and wetting resistance in membrane distillation. *ACS Applied Materials & Interfaces*, *12*(18), 20942–20954. https://doi.org/10.1021/acsami.0c03577

Wang, Z. L. (2004). Zinc oxide nanostructures: Growth, properties and applications. *Journal of Physics Condensed Matter*, *16*(25), 829-858. https://doi.org/10.1088/0953-8984/16/25/R01 AQ17

Wei, X., Zhao, B., Li, X. M., Wang, Z., He, B. Q., He, T., & Jiang, B. (2012). CF 4 plasma surface modification of asymmetric hydrophilic polyethersulfone membranes for direct contact membrane distillation. *Journal of Membrane Science*, *407–408*, 164–175. https://doi.org/10.1016/j.memsci.2012.03.031

Wenzel, R. N. (1936). Resistance of solid surfaces to wetting by water. *Industrial & Engineering Chemistry*, *28*(8), 988–994. https://doi.org/10.1021/ie50320a024

Woo, Y. C., ~~&~~ Kim, Y., Shim, W. G., Tijing, L. D., Yao, M., Nghiem, L. D., Choi J. S., Kim S. H., Shon, H. K. (2016). *Graphene/PVDF flat-sheet membrane for the treatment of RO brine from coal seam gas produced water by air gap membrane distillation*. *Journal of Membrane Science*, *513*, 74–84. https://doi.org/10.1016/j.memsci.2016.04.014

Woo, Y. C., Tijing, L. D., Shim, W.-G., Choi, J.-S., Kim, S.-H., He, T., Drioli, E., & Shon, H. K. (2016). Water desalination using graphene-enhanced electrospun nanofiber membrane via air gap membrane distillation. *Journal of Membrane Science*, *520*, 99–110. https://doi.org/10.1016/j.memsci.2016.07.049

Xiao, Z., Zheng, R., Liu, Y., He, H., Yuan, X., Ji, Y., Li, D., Yin, H., Zhang, Y., Li, X.-M., & He, T. (2019). Slippery for scaling resistance in membrane distillation: A novel porous micropillared superhydrophobic surface. *Water Research*, *155*, 152–161. https://doi.org/10.1016/j.watres.2019.01.036

Xu, B., Zheng, Q., Song, Y., & Shangguan, Y. (2006). Calculating barrier properties of polymer/clay nanocomposites: Effects of clay layers. *Polymer*, *47*(8), 2904–2910. https://doi.org/10.1016/j.polymer.2006.02.069

Yan, L., Li, Y. S., Xiang, C. B., & Xianda, S. (2006). Effect of nano-sized Al2O3-particle addition on PVDF ultrafiltration membrane performance. *Journal of Membrane Science*, *276*(1–2), 162–167. https://doi.org/10.1016/j.memsci.2005.09.044

Yang, C., Li, X.-M., Gilron, J., Kong, D-f., Yin, Y., Oren, Y., Linder, C., & He, T. (2014). CF4 plasma-modified superhydrophobic PVDF membranes for direct contact membrane distillation *Journal of Membrane Science*, *456*, 155–161. https://doi.org/10.1016/j.memsci.2014.01.013

Yang, C., Tian, M., Xie, Y., Li, X. M., Zhao, B., He, T., & Liu, J. (2015). Effective evaporation of CF4 plasma modified PVDF membranes in direct contact membrane distillation *Journal of Membrane Science*, *482*, 25–32. https://doi.org/10.1016/j.memsci.2015.01.059

Yang, X., Wang, R., Shi, L., Fane, A. G., & Debowski, M. (2011). Performance improvement of PVDF hollow fiber-based membrane distillation process. *Journal of Membrane Science*, *369*(1–2), 437–447.

https://doi.org/10.1016/j.memsci.2010.12.020

Yao, M., Tijing, L. D., Naidu, G., Kim, S. H., Matsuyama, H., Fane, A. G., & Shon, H. K. (2020). A review of membrane wettability for the treatment of saline water deploying membrane distillation. *Desalination*, *479*, 114312. https://doi.org/10.1016/j.desal.2020.114312 AQ18

Yin, J., & Deng, B. (2015). Polymer-matrix nanocomposite membranes for water treatment. *Journal of Membrane Science*, *479*, 256–275. https://doi.org/10.1016/j.memsci.2014.11.019

Yin, Y., Jeong, N.-Y., & Tong, T. (2020). The effects of membrane surface wettability on pore wetting and scaling reversibility associated with mineral scaling in membrane distillation. *Journal of Membrane Science*, *614*, 118503. https://doi.org/10.1016/j.memsci.2020.118503

Yue, R., Meng, D., Ni, Y., Jia, Y., Liu, G., Yang, J., Liu, H., Wu, X., & Chen, Y. (2013). One-step flame synthesis of hydrophobic silica nanoparticles. *Powder Technology*, *235*, 909–913. https://doi.org/10.1016/j.powtec.2012.10.021

Zeyu, M., Hong, Y., Liyuan, M., & Su, M. (2009). Superhydrophobic membranes with ordered arrays of nanospiked microchannels for water desalination. *Langmuir: The ACS Journal of Surfaces and Colloids*, *25*(10), 5446–5450. https://doi.org/10.1021/la900494u

Zhang, J., Dow, N., Duke, M., Ostarcevic, E., Li, J. De., & Gray, S. (2010). Identification of material and physical features of membrane distillation membranes for high performance desalination. *Journal of Membrane Science*, *349*(1–2), 295–303. https://doi.org/10.1016/j.memsci.2009.11.056

Zhang, J., Song, Z., Li, B., Wang, Q., & Wang, S. (2013). Fabrication and characterization of superhydrophobic poly (vinylidene fluoride) membrane for direct contact membrane distillation. *Desalination*, *324*, 1–9. https://doi.org/10.1016/j.desal.2013.05.018

Zhang, Y., & Wang, R. (2013). Fabrication of novel polyetherimide-fluorinated silica organic-inorganic composite hollow fiber membranes intended for membrane contactor application. *Journal of Membrane Science*, *443*, 170–180. https://doi.org/10.1016/j.memsci.2013.04.062

Zhou, R., Rana, D., Matsuura, T., & Lan, C. Q. (2019). Effects of multi-walled carbon nanotubes (MWCNTs) and integrated MWCNTs/SiO2 nano-additives on PVDF polymeric membranes for vacuum membrane distillation *Separation and Purification Technology*, *217*, 154–163. https://doi.org/10.1016/j.seppur.2019.02.013

Zhu, H., Wang, H., Wang, F., Guo, Y., Zhang, H., & Chen, J. (2013). Preparation and properties of PTFE hollow fiber membranes for desalination through vacuum membrane distillation. *Journal of Membrane Science*, *446*, 145–153. https://doi.org/10.1016/j.memsci.2013.06.037

Zhu, W., Liu, Y., Guan, K., Peng, C., Qiu, W., & Wu, J. (2019). Integrated preparation of alumina microfiltration membrane with super permeability and high selectivity. *Journal of the European Ceramic Society*, *39*(4), 1316–1323. https://doi.org/10.1016/j.jeurceramsoc.2018.10.022

Zhu, Y., Liu, X., Hu, Y., Wang, R., Chen, M., Wu, J., Wang, Y., Kang, S., Sun, Y., & Zhu, M. (2019). Behavior, remediation effect and toxicity of nanomaterials in water environments. *Environmental Research*, *174*, 54–60. https://doi.org/10.1016/j.envres.2019.04.014

Nomenclature

AGMD	air gap membrane distillation
B	geometric factor determined by pore structure
CNT	carbon nanotube
	FAS fluoroalkylsilane
GO	graphene oxide
LEP	liquid entry pressure
M	molecular weight
MD	membrane distillation
MMM	mixed matrix membranes
PcH	Polyvinylidene fluoride-co-hexafluoropropylene
PP	polypropylene
PTFE	polytetrafluoroethylene
PVDF	poly (vinylidene fluoride)
RO	reverse osmosis
	SDS Sodium Dodecyl Sulfate
VMD	vacuum membrane distillation
γ	surface tension
d	pore diameter
ε	porosity
λ	heat of vaporization
τ	tortuosity
δ	membrane thickness

Author Query

1. **Query:** [AQ0] - : Please review the table of contributors below and confirm that the first and last names are structured correctly and that the authors are listed in the correct order of contribution. This check is to ensure that your names will appear correctly online and when the article is indexed.

Sequence	Prefix	Given name(s)	Surname	Suffix
1		Emilia	Gontarek	
2		Roberto	Castro-Muñoz	
3		Marek	Lieder	

Response: [*Author: emilia.gontarek@pg.edu.pl*]: Answered within text

2. **Query:** [AQ1] - : Please check if the affiliations are OK as typeset.
Response: [*Author: emilia.gontarek@pg.edu.pl*]: Ok

3. **Query:** [AQ2] - : Please provide physical address for the corresponding authors.
Response: [*Author: emilia.gontarek@pg.edu.pl*]: CONTACT Emilia Gontarek-Castro emilia.gontarek@pg.edu.pl; Faculty of Chemistry, Department of Process Engineering and Chemical Technology, Gdansk University of Technology, Gdansk, Poland; Roberto Castro-Muñoz food.biotechnology88@gmail.com; castromr@tec.mx; Tecnologico de Monterrey, Campus Toluca, Avenida Eduardo Monroy Cárdenas 2000 San Antonio Buenavista, Toluca de Lerdo, Mexico

4. **Query:** [AQ3] - : Please provide complete details for (Chen et al., 2014; Guo et al., 2014 and Gryta 2019) in the reference list or delete the citation from the text.
Response: [*Author: emilia.gontarek@pg.edu.pl*]: Answered within text

5. **Query:** [AQ4] - : The disclosure statement has been inserted. Please correct if this is inaccurate.
Response: [*Author: emilia.gontarek@pg.edu.pl*]: Ok

6. **Query:** [AQ5] - : Please provide title of the patent and publisher name for Ref. Bodell (1963).
Response: [*Author: emilia.gontarek@pg.edu.pl*]: B.R. Bodell, Silicon rubber vapour diffusion in saline water distillation, United States Patent Serial No. 285,032, 1963.

7. **Query:** [AQ6] - : The year of publication has been changed as per Crossref details both in the list and in the text for Ref. Castro-Muñoz et al. (2019). Please check.
Response: [*Author: emilia.gontarek@pg.edu.pl*]: Ok

8. **Query:** [AQ7] - : Please differentiate Refs. Castro-Muñoz et al. (2019); Liao et al. (2013, 2014); Nthunya et al. (2019); Zhu et al. (2019) with subsequent authors name to differentiate them in text citations.
Response: [*Author: emilia.gontarek@pg.edu.pl*]: Answered within text

9. **Query:** [AQ8] - : Please check if citations of Ref. Chen et al. (2016) are OK as given.
Response: [*Author: emilia.gontarek@pg.edu.pl*]: Ok

10. **Query:** [AQ9] - : There is no mention of (Gryta 2018, Guo & Mei 2014) in the text. Please insert a citation in the text or delete the reference as appropriate.
Response: [*Author: emilia.gontarek@pg.edu.pl*]: Answered within text ↑

11. **Query:** [AQ10] - : The year of publication has been changed as per Crossref details both in the list and in the text for Ref. Horseman et al. (2021). Please check.
Response: [*Author: emilia.gontarek@pg.edu.pl*]: Ok ↑

12. **Query:** [AQ11] - : Please provide complete details for Refs. Kumar et al. (2020); Woo & Kim (2016).
Response: [*Author: emilia.gontarek@pg.edu.pl*]: Answered within text ↑

13. **Query:** [AQ12] - : Please provide the journal title for Ref. Larbot et al. (2004).
Response: [*Author: emilia.gontarek@pg.edu.pl*]: Answered within text ↑

14. **Query:** [AQ13] - : The year of publication has been changed as per Crossref details both in the list and in the text for Ref. Movafeghi et al. (2018). Please check.
Response: [*Author: emilia.gontarek@pg.edu.pl*]: Ok ↑

15. **Query:** [AQ14] - : Please provide the journal title for Ref. Onda et al. (1996).
Response: [*Author: emilia.gontarek@pg.edu.pl*]: Answered within text ↑

16. **Query:** [AQ15] - : Please provide the volume number and page range for Ref. Su et al. (2019).
Response: [*Author: emilia.gontarek@pg.edu.pl*]: Answered within text ↑

17. **Query:** [AQ16] - : Please provide the page range for Ref. Suresh et al. (2018).
Response: [*Author: emilia.gontarek@pg.edu.pl*]: Answered within text ↑

18. **Query:** [AQ17] - : Please provide the page range for Ref. Wang (2004).
Response: [*Author: emilia.gontarek@pg.edu.pl*]: Answered within text ↑

19. **Query:** [AQ18] - : Please note that Yao et al., 2020 seems to be repeated twice in the reference list. Hence the latter has been deleted and citations have been changed accordingly. Please correct if inaccurate.
Response: [*Author: emilia.gontarek@pg.edu.pl*]: Ok ↑

20. **Query:** [AQ19] - : Please provide missing citation(s) for Figure 9.
Response: [*Author: emilia.gontarek@pg.edu.pl*]: Answered within text ↑

21. **Query:** [AQ20] - : Please note that the ORCID section has been created from information supplied with your manuscript submission/CATS. Please correct if this is inaccurate.
Response: [*Author: emilia.gontarek@pg.edu.pl*]: Is it possible to connect others authors names with their ORCID account? Roberto Castro-Muñoz 0000-0002-7657-3302 Marek Lieder 0000-0001-7410-5161 ↑

Comments

1. **Comments [Author - 1/22/2021 2:07:21 PM]:** Gontarek-Castro

2. **Comments [Author - 1/22/2021 2:08:10 PM]:** Gontarek-Castro

3. **Comments [Author - 1/22/2021 7:58:34 PM]:** Figure 5 was supposed to be placed here. Likewise, all subsequent ones are incorrectly placed.